Published by
NIGERIAN SOCIETY OF PHYSICAL SCIENCES
Available online @ https://journal.nsps.org.ng/index.php/jnsps

J. Nig. Soc. Phys. Sci. 7 (2025) 2323

Journal of the Nigerian Society of Physical Sciences

A numerical algorithm based on extended cubic B-spline functions for solving time-fractional convection-diffusion-reaction equation with variable coefficients

Anthony Anya Okeke [a,d,*], Nur Nadiah Abd Hamid [b], Wen Eng Ong [a], Muhammad Abbas [c]

[a] School of Mathematical Sciences, Universiti Sains Malaysia, 11800 Penang, Malaysia
[b] Nur Nadiah Academic Services, 13800 Butterworth, Penang, Malaysia
[c] Department of Mathematics, University of Sargodha, Sargodha, Pakistan
[d] Department of Mathematics, Federal University Gashua, P.M.B. 1005 Gashua, Yobe State, Nigeria

Abstract

In this research, we develop an innovative and efficient numerical method for solving a nonlinear one-dimensional time-fractional convection-diffusion-reaction equation (TFCDRE) with a variable coefficient. This method integrates the Crank-Nicolson finite difference scheme with extended cubic B-spline (ExCBS) basis functions. The Caputo fractional derivative is applied for temporal discretization, while the ExCBS functions are utilized for spatial discretization. The stability of the method was discussed by the von Neumann method, which shows unconditional stability; and the convergence analysis secure an order of $O(h^2 + \triangle t^{2-\alpha})$. We demonstrated the efficiency and simplicity of our method through three numerical experiments and verified its accuracy using the absolute error (L_2) and maximum error (L_∞) norms in temporal and spatial dimensions. The results are also graphically represented and show substantial agreement with the approximated and exact solution. We confirmed the effectiveness and accuracy of our approach over the local discontinuous Galerkin finite element and the compact finite difference methods, respectively, from the literature.

DOI:10.46481/jnsps.2025.2323

Keywords: Caputo fractional derivative, Crank–Nicolson finite difference formulation, Time fractional convection-diffusion-reaction equation, Extended cubic B-spline basis functions, Stability and convergence

Article History :
Received: 25 August 2024
Received in revised form: 02 October 2024
Accepted for publication: 02 October 2024
Available online: 30 October 2024

Communicated by: Joel Ndam

1. Introduction

Partial differential equations (PDEs) serve as powerful tools for modelling a wide array of natural phenomena, including medical issues. Solutions to PDEs, in conjunction with initial and boundary conditions, are crucial for accurately modelling anomalous (convection/diffusion) phenomena across diverse fields, including biology, chemistry, geology, physics, economics, and engineering. However, the PDEs of integer-order variables are extensively utilized in broad-range applications. In recent times, fractional derivatives have been developing and are increasingly being applied to real-world problems owing to their inherent non-local properties. Fractional partial

*Corresponding author Tel. No.: +234-803-052-3185.
Email address: anyaokeke@gmail.com (Anthony Anya Okeke)

differential equations (FPDEs) have exceedingly practical applications in engineering, science, and financial modelling, offering new perspectives and solutions in these disciplines [1–4].

Research has shown that FPDEs are more effective than traditional integer-order PDEs in capturing the memory and hereditary characteristics of different physical materials and processes. In the same vein, FPDEs are also good and appropriate tools for modelling and describing certain natural and non-natural phenomena, for example, convection and diffusion processes, wave, ion acoustic wave, groundwater flow and Geo-Hydrology, visco-elasticity, fluid mechanics, fractal network, cybernetics, astrophysics, signal processes, rheology, COVID-19 model, and fractal media, among others [1, 5–8]. There are ample competing definitions of fractional differentiation and integration [9]. The ones commonly employed by researchers are Grünwald-Letnikov, Riemann-Liouville, Caputo, Hadamard, and the Atangana-Baleanu derivative. These definitions differ in their properties, and mathematical formulations, and each has advantages and disadvantages depending on the specific application. It has been observed that problems occurring in the theory of fractional differintegrals are extremely important, very demanding, and require extraneous mathematical techniques.

The quest for an efficient and accurate numerical approach to examine FPDEs has led to the development of numerical solutions for nonlinear time-fractional convection-diffusion-reaction equation (TFCDRE) with variable coefficients. The equation is so advantageous and essential in mathematical modelling as it has numerous applications in engineering and natural sciences such as the modelling of semiconductors, food processing, oil reservoir flow transport, modelling of biological systems, groundwater pollution systems, the transport of air, and the reaction of chemical species among others [10–13]. In the present research, we considered the following time-fractional convection-diffusion-reaction model (equation (1)):

$$\frac{\partial^{\alpha} p(r,t)}{\partial t^{\alpha}} + v_1(r)\frac{\partial p(r,t)}{\partial r} - v_2(r)\frac{\partial^2 p(r,t)}{\partial r^2} + v_3(r)p(r,t) = g(r,t), \quad r \in \Omega,\ t \in (0,T), \tag{1}$$

with respect to the initial and end conditions stated by equations (2) and (3), respectively,

$$p(r,0) = \varphi_1(r), \quad a \le r \le b, \tag{2}$$

$$p(a,t) = \varphi_2(t), \quad p(b,t) = \varphi_3(t), \quad t \ge 0, \tag{3}$$

where the coefficients v_1, v_2 and v_3 are functions depending on r, $v_3(r) \ge 0$, $\Omega \subset \Re$ a bounded domain, $\varphi_1(r)$, $\varphi_2(t)$, $\varphi_3(t)$ are given functions, $g(r,t)$ the source term and $\partial^{\alpha} p(r,t) \div \partial t^{\alpha}$ represents the Caputo's fractional derivative (CFD) of order $\alpha \in [0,1]$, $\Omega = (0,1) \times (0,T]$. Meanwhile, the interval $[0,1]$ is chosen to normalize the spatial domain while the bounded domain $\Omega = (0,1)$ is selected to ensures that the mathematical model remains well-defined and avoids complications associated with unbounded domains. Outside the interval, $r \notin [0,1]$, the solution is generally undefined for this problem setup and complications can arise that may hinder both theoretical analysis and practical applications.

Like every other FPDE, one of the challenges in solving TFCDEs is that these equations often lack analytical solutions. Thus, numerical methods provide an alternative tool for solving TFCDRE under the prescribed conditions. We noticed that researchers have developed and propagated advanced numerical techniques in solving the TFCDREs. This includes Wang and Ren [14], who proposed a compact finite difference method (FDM) for solving a class of TFCDREs with variable coefficients. A collocation technique with fractional powers exponential trial functions was employed by Liu and Chang [15] to solve numerically singularly perturbed 2D fractional convection-diffusion-reaction equations (CDREs). Li and Wang [16] reviewed and developed many numerical techniques to solve TFCDRE of Caputo's derivatives focusing on their stability and convergence.

A weak Galerkin finite element method (FEM) was proposed by Toprakseven [17] for solving TFCDRE, while in Ngondiep [18], the author suggested a two-level fourth-order numerical scheme for solving TFCDREs with various initial and boundary conditions. Choudhary *et al* [19] solved the time-FPDEs with a time delay extended to CDRE using FDM. In Naeem *et al.* [20], they combined the Elzaki transform with the homotopy perturbation method (HPM) to secure the numerical solution of the fractional-order CDRE using the Elzake Atangana-Baleanu operator. Yasmin [21] employed the combination of Aboodh transformation and HPM to obtain the analytical approximation of the fractional-order CDRE comprising fractional Atangana-Baleanu and Caputo operators. A virtual element method was suggested by Zhang and Feng [22] to examine the 2D TFCDREs of CFD with non-smooth data.

These days, there are vast computational and analytical approximation techniques for solving FPDEs like the FDM, the FEM, the Laplace decomposition method, the hybrid/modified explicit group method, the Invariant subspace method, the HPM, Jacobi operational matrix, and the Hermite wavelet method [23–29]. Nevertheless, the application of these methods is constrained by the substantial computational expenses of mesh generation. To overcome this, B-spline techniques emerged due to their flexibility and straightforward implementation. B-splines are mathematical functions constructed using a set of control points, a specific degree, and a knot vector. The shape of the resulting curve or surface is determined by the knot vector, which is a sequence of ordered variables. The degree of the B-spline corresponds to the highest degree of the polynomial used in each piecewise segment of the curve.

Some applications of B-spline basis functions can be found in Yaseen and Abbas [30] which suggested cubic trigonometric B-splines (CTBS) to determine the time-fractional (TF) Burgers' equation. Also, Shafiq *et al.* [31] used cubic B-spline (CBS) to solve TF advection-diffusion equation with Atangana–Baleanu derivative. The authors in [32] secured a numerical approach to solve the TF diffusion equation by quintic B-spline basis while Okeke *et al.* [33] employed CBS to discuss a certain TF Navier-Stokes equation with Caputo operator. A fourth-order optimal CBS collocation method was engaged by Roul and Goura [34] to determine nonhomogeneous TF diffusion equations. Abbas *et al.* [35] suggested a numerical method

based on CBS to resolve third-order TF differential equations.

The extended cubic B-spline (ExCBS) was employed by Umar *et al.* [36] to discuss the approximate solution of the Atangana-Baleanu TF advection-diffusion equation as Hadhoud *et al.* [37] utilized the CTBS function and Crank-Nicolson scheme in solving the TF Schrödinger equation. Fractional coupled Burgers equations involving exponential kernels were solved by Akram *et al.* [38] using ExCBS. Ghafoor *et al.* [39] suggested a technique that used CBS collocation to resolve the numerical solution coupled viscous Burgers equation of fractional order with CFD. Other B-spline applications can be found in Refs. [40–44]. To our knowledge, the ExCBS method has not yet been employed to solve the TFCDRE. This enables us to offer an original contribution by applying the ExCBS technique to this specific FPDE model. Therefore, our main goal in this work is to develop and discuss an efficient numerical method for solving nonlinear TFCDREs with variable coefficients using ExCBS. Specifically, we will focus on the stability, convergence, accuracy, and computational efficiency of the proposed scheme. The structure of the paper is as follows: Section 2 provides preliminaries. Sections 3 and 4 cover the ExCBS and the description of our proposed scheme. Sections 5 and 6 address the stability and convergence analysis. Section 7 presents three numerical examples and their discussions, while section 8 is the conclusion.

2. Preliminaries

Definition 1. The CFD $\frac{\partial^\alpha p(r,t)}{\partial t^\alpha}$ of a given function $p(r,t)$, employed in this research is defined in Ref. [45] as

$$\frac{\partial^\alpha p(r,t)}{\partial t^\alpha} = \begin{cases} \frac{1}{\Gamma(n-\alpha)} \int_0^t \frac{\partial^n p}{\partial s^n}(t-s)^{n-\alpha-1} ds, & n-1 < \alpha < n, \\ {}^cD_t^\alpha p(r,t), & \alpha = n \in \mathbb{N}, \end{cases} \tag{4}$$

where Γ is the Euler's Gamma function.

$$\frac{\partial^\alpha p(r,t)}{\partial t^\alpha} = \begin{cases} \frac{1}{\Gamma(n-\alpha)} \int_0^t \frac{\partial^n p}{\partial s^n}(t-s)^{n-\alpha-1} ds, & n-1 < \alpha < n, \\ {}^cD_t^\alpha p(r,t), & \alpha = n \in \mathbb{N}. \end{cases} \tag{5}$$

2.1. Parseval's identity

If $\tilde{p} \in L^2[a,b]$, then Parseval's identity is defined in [46] as

$$\sum_{n=-\infty}^{\infty} |\hat{p}(n)|^2 = \int_a^b |\tilde{w}(r)|^2 dr, \tag{6}$$

where $\hat{p}(n) = \int_a^b \tilde{p}(r) e^{2\pi i n s} dr$ for all integer n is its Fourier transform

2.2. Extended Cubic B-spline Functions

Presume that $N \in \mathbb{Z}^+$ and the space interval $[a,b]$ is equally spaced partition of step length $h = r_{j+1} - r_j = b - a \div N$, such that $a = r_0 < r_1 < \cdots < r_N = b$, with $r_j = r_0 + jh,\ j = 0:1:N$. Then the ExCBS basis function can be defined as in Eq. (7) [47]:

$$B_j(r,\beta) = \frac{1}{24h^4} \begin{cases} 4h(1-\beta)(r-r_{j-2}) & \\ +3\beta(r-r_{j-2})^4, & r \in [r_{j-2}, r_{j-1}), \\ Q^* - 3\beta(r-r_{j-1})^4 & \\ -12(r-r_{j-1})^3 h, & r \in [r_{j-1}, r_j), \\ Q^{**} - 12(r_{j+1}-r)^3 h & \\ -3\beta(r_{j+1}-r), & r \in [r_j, r_{j+1}), \\ 4(1-\beta)(r_{j+2}-r)^3 h & \\ +3\beta(r_{j+2}-r)^4, & r \in [r_{j+1}, r_{r+2}) \\ 0, & \text{otherwise}, \end{cases} \tag{7}$$

where $Q^* = (4-\beta)h^4 + 12(r-r_{j-1})h^3 + 6(2+\beta)(r-r_{j-1})^2h^2$, $Q^{**} = h^4(4-\beta) + 12(r_{j+1}-1)h^3 + 6(2+\beta)(r_{j+1}-r)^2h^2$, $j = -1(1)N+1, r \in \mathbb{R}$ is a variable and also $\beta \in \mathbb{R}$ is a free parameter and $\beta \in [-8,1]$. If $\beta = 0$ the ExCBS is reduced to CBS. Furthermore, ExCBS shares several characteristics with CBS, including geometric invariability, local support, symmetry, non-negativity, convex hall property, and the partition of unity. The spline set $\{B_{-1}, B_0, \cdots, B_N, B_{N+1}\}$ engaged as a basis over the assumed domain $[a,b]$. Presume that $p(r,t)$ is a satisfactorily smooth function, then we have an ExCBS that executes the approximated solution as:

$$P(r,t) = \sum_{j=-1}^{N+1} S_j(t) B_j(r,\beta), \tag{8}$$

where $S_j(t)$'s are the undetermined coefficients to be calculated. The approximate solution $P(r_j,t^n) = P_j^n$ of the systems, equation (8) including its first and second derivatives can be represented as:

$$\begin{cases} P_j^n = a_1 S_{j-1}^n + a_2 S_j^n + a_1 S_{j+1}^n, \\ (P_r)_j^n = -b_1 S_{j-1}^n + b_2 S_j^2 + b_1 S_{j+1}^n, \\ (P_{rr})_j^n = c_1 S_{j-1}^n + c_2 S_j^n + c_1 S_{j+1}^n, \end{cases} \tag{9}$$

where $a_1 = \frac{4-\beta}{24}$, $a_2 = \frac{32+4\beta}{48}$, $b_1 = \frac{1}{2h}$, $b_2 = 0$, $c_1 = \frac{8+4\beta}{8h^2}$, and $c_2 = \frac{-4-2\beta}{2h^2}$.

3. Description of the scheme

We employed the finite difference method to discretize the time CFD of the first order as defined in Eq. (1). Presume the time interval $[0,T]$, the knots $0 = t_0 < t_1 < \cdots < t_N = T$, the temporal step size $t_n = n\Delta t$ for $n = 0(1)N$ at $\Delta t = T \div N$, and the final time T. Then the CFD of $\alpha \in (0,1)$ of TFCDRE discretized at $t = t_{n+1}$ is presented in system, equation (10)

Table 1. A comparison of the exact and approximate solutions of Example 1 with $\beta = 0.00012$, $\triangle t = 0.01$, and time $T = 1$.

r	Exact	Approximate Solution		Absolute Error	
		$\alpha = 0.65$ N=80	$\alpha = 0.35$ N=100	$\alpha = 0.65$ N=80	$\alpha = 0.35$ N=100
0.1	0.38	0.380139	0.380005	0.000139321	0.00000524797
0.2	0.72	0.720283	0.720012	0.000283369	0.0000122845
0.3	1.02	1.020420	1.020020	0.000419995	0.0000200413
0.4	1.28	1.280540	1.280030	0.000535637	0.0000273824
0.5	1.50	1.500620	1.500030	0.000615436	0.0000331111
0.6	1.68	1.680640	1.680040	0.000643836	0.0000360072
0.7	1.82	1.820610	1.820030	0.000605835	0.0000349070
0.8	1.92	1.920490	1.920030	0.000489031	0.0000288365
0.9	1.98	1.980290	1.980020	0.000286453	0.0000171983

Table 2. Absolute numerical errors for Example 1 with $\triangle t = 0.01$, $\beta = 0.000055$, and $T = 0.1$.

r	$\alpha = 0.9$	$\alpha = 0.7$	$\alpha = 0.5$	$\alpha = 0.3$	$\alpha = 0.1$
0.1	7.66471E-04	2.06083E-04	4.76755E-05	5.99821E-06	4.10318E-06
0.2	1.55063E-03	4.17458E-04	9.71613E-05	1.28948E-05	7.52774E-06
0.3	2.28934E-03	6.16821E-04	1.44213E-04	1.99010E-05	1.02213E-05
0.4	2.91191E-03	7.84796E-04	1.84097E-04	2.61598E-05	1.20967E-05
0.5	3.34039E-03	9.00093E-04	2.11638E-04	3.07541E-05	1.30360E-05
0.6	3.49232E-03	9.40361E-04	2.21439E-04	3.27405E-05	1.29048E-05
0.7	3.28704E-03	8.83998E-04	2.08328E-04	3.12208E-05	1.15750E-05
0.8	2.65622E-03	7.13094E-04	1.68072E-04	2.54553E-05	8.95970E-06
0.9	1.55888E-03	4.17536E-04	9.83630E-05	1.50207E-05	5.05717E-06

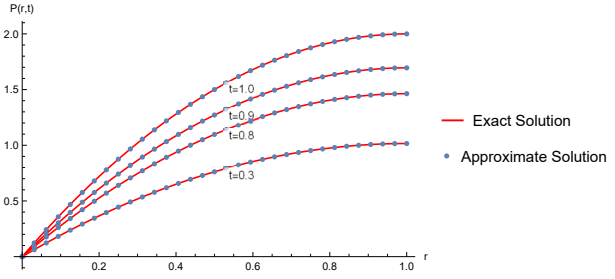

Figure 1. Comparison plot of exact and approximate solutions with $N = 32$, $\alpha = 0.45$, $\triangle t = 0.01$ for Example 1 at different time levels.

$$
\begin{aligned}
\frac{\partial^\alpha p(r,t_{n+1})}{\partial t^\alpha} &= \frac{1}{\Gamma(1-\alpha)}\int_0^{t_{n+1}} \frac{\partial p(r,s)}{\partial s}\cdot\frac{ds}{(t_{n+1}-s)^\alpha},\\
&= \frac{1}{\Gamma(1-\alpha)}\sum_{l=0}^{n}\int_{t_l}^{t_{l+1}} \frac{\partial p(r,s)}{\partial s}\cdot\frac{ds}{(t_{n+1}-s)^\alpha},\\
&= \frac{1}{\Gamma(1-\alpha)}\sum_{l=0}^{n}\frac{p(r,t_{l+1})-p(r,t_l)}{\Delta t}\int_{t_l}^{t_{l+1}}\frac{ds}{(t_{n+1}-s)^\alpha}+S_{\Delta t}^{n+1},\\
&= \frac{1}{\Gamma(1-\alpha)}\sum_{l=0}^{n}\frac{p(r,t_{l+1})-p(r,t_l)}{\Delta t}\int_{t_{n-l}}^{t_{n+1-l}}\frac{d\tau}{\tau^\alpha}+S_{\Delta t}^{n+1},\\
&= \frac{1}{\Gamma(1-\alpha)}\sum_{l=0}^{n}\frac{p(r,t_{n+1-l})-p(r,t_{n-l})}{\Delta t}\int_{t_l}^{t_{l+1}}\frac{d\tau}{\tau^\alpha}+S_{\Delta t}^{n+1},\\
&= \frac{1}{\Gamma(1-\alpha)}\sum_{l=0}^{n}\frac{p(r,t_{n+1-l})-p(r,t_{n-l})}{\Delta t^\alpha}\left(\frac{(l+1)^{1-\alpha}-l^{1-\alpha}}{1-\alpha}\right)+S_{\Delta t}^{n+1},\\
\frac{\partial^\alpha p(r,t_{n+1})}{\partial t^\alpha} &= \frac{1}{\Gamma(2-\alpha)}\sum_{l=0}^{n} w_l\frac{p(r,t_{n+1-l})-p(r,t_{n-l})}{\Delta t^\alpha}+S_{\Delta t}^{n+1},
\end{aligned}
\tag{10}
$$

where $w_l = (l+1)^{1-\alpha} - l^{1-\alpha}$, $\tau = (t_{n+1} - s)$. Additionally, the truncation error $S_{\Delta t}^{n+1}$, discussed in Ref. [48] is presented as

$$
|S_{\Delta t}^{n+1}| \le c_p \Delta t^{2-\alpha}, \tag{11}
$$

where c_p is a constant.

Remark. The following properties of the coefficient w_l are easily observed:

- $w_l > 0, \quad l = 0, 1, 2, \ldots, n,$
- $1 = w_0 > w_1 > w_2 > \ldots > w_l, \quad w_l \to 0, \text{ as } l \to \infty,$
- $\sum_{l=0}^{n}(w_l - w_{l+1}) + w_{l+1} = (1 - w_1) + \sum_{l=1}^{n-1}(w_l - w_{l+1}) + w_n = 1.$

Utilizing Eq. (10) and employing the $\theta-$weighted scheme, Eq. (1) attains the form

$$
\begin{aligned}
&\alpha_0 p^{n+1} + \theta[v_1(r)p_r^{n+1} - v_2(r)p_{rr}^{n+1} + v_3(r)p^{n+1}]\\
&\quad = \alpha_0 p^n - (1-\theta)[v_1(r)p_r^n - v_2(r)p_{rr}^n + v_3(r)p^n]\\
&\quad - \alpha_0\sum_{l=1}^{n} w_l[p^{n+1-l} - p^{n-l}] + g^{n+1}, \quad (n = 0:1:N).
\end{aligned}
\tag{12}
$$

The system, equation (12) transforms to explicit for $\theta = 0$, fully implicit for $\theta = 1$ and Crank-Nicolson for $\theta = 0.5$, respectively. Substituting Eq. (9) into Eq. (12), we obtain Eq. (13):

$$
\begin{aligned}
&(\alpha_0 a_1 - \theta v_1(r)b_1 - \theta v_2(r)c_1 + \theta v_3(r)a_1)S_{j-1}^{n+1}\\
&\quad + (\alpha_0 a_2 + \theta v_1(r)b_2 - \theta v_2(r)c_2 + \theta v_3(r)a_2)S_j^{n+1}\\
&\quad + (\alpha_0 a_1 + \theta v_1(r)b_1 - \theta v_2(r)c_1 + \theta v_3(r)a_1)S_{j+1}^{n+1}
\end{aligned}
$$

Table 3. Error norms for Example 1 for $T = 0.1$, $N = 80$.

α	$\triangle t$	β	Method in [14]		Proposed Method		Order
			L_2	L_∞	L_2	L_∞	
	1/20	0.0000121	9.9166E-05	1.7367E-04	7.9174E-05	1.2634E-05	$\cdots$
	1/40	0.000012	2.5350E-05	4.4337E-05	2.1607E-05	3.4879E-06	1.8569
0.25	1/80	0.000016	6.4247E-06	1.1227E-05	5.4452E-06	8.3929E-07	2.0551
	1/160	0.000022	1.6197E-06	2.8285E-06	1.2662E-06	2.1351E-07	1.9748
	1/320	0.00000145	4.0703E-07	7.1051E-07	3.1678E-07	5.0734E-08	1.9986

$$
\begin{aligned}
&= \alpha_0[a_1S_{j-1}^n + a_2S_j^n + a_1S_{j+1}^n] - \alpha_0\sum_{l=1}^{n} w_l(a_1[S_{j-1}^{n+1-l} - S_{j-1}^{n-l}] \\
&\quad + a_2[S_j^{n+1-l} - S_j^{n-l}] + a_1[S_{j+1}^{n+1-l} - S_{j+1}^{n-l}]) \\
&\quad - (1-\theta)[(-v_1(r)b_1 - v_2(r)c_1 + v_3(r)a_1)S_{j-1}^n \\
&\quad + (v_1(r)b_2 - v_2(r)c_2 + v_3(r)a_2)S_j^n \\
&\quad + (v_1(r)b_1 - v_2(r)c_1 + v_3(r)a_1)S_{j+1}^n] + g_j^{n+1}, \\
&\qquad j = 0, 1, 2, \cdots, N. \qquad (13)
\end{aligned}
$$

The system, equation (13) of $(N+1)$ linear equations in $(N+3)$ unknowns $(S_{-1}, S_0, e_1, \cdots, S_{N+1})^T$ can be secured. To attain the unique solution, the boundary conditions, equation (3) are engaged.

$$a_1S_{-1}^{n+1} + a_2S_0^{n+1} + a_1S_1^{n+1} = \varphi_2(t^{n+1}), \qquad (14)$$

$$a_1S_{N-1}^{n+1} + a_2S_N^{n+1} + a_1S_{N+1}^{n+1} = \varphi_3(t^{n+1}). \qquad (15)$$

The system then becomes

$$AS^{n+1} = -DS^n + B(\alpha_0 w_n S^0 + \alpha_0 \sum_{l=0}^{n-1}(w_l - w_{l+1})S^{n-l}) + G, \qquad (16)$$

where

$$A = \begin{bmatrix} a_1 & a_2 & a_1 & & \cdots & \cdots & 0 \\ u_1 & u_2 & u_3 & & \cdots & \cdots & 0 \\ & u_1 & u_2 & u_3 & \ldots & \cdots & 0 \\ & & & & \ddots & \ddots & \vdots \\ \vdots & \cdots & u_1 & u_2 & u_3 & & \\ \vdots & \cdots & & u_1 & u_2 & u_3 & \\ 0 & \cdots & & & a_1 & a_2 & a_1 \end{bmatrix},$$

$$D = \begin{bmatrix} 0 & 0 & 0 & & \cdots & \cdots & 0 \\ z_1 & z_2 & z_3 & & \cdots & \cdots & 0 \\ & z_1 & z_2 & z_3 & \ldots & \cdots & 0 \\ & & & & \ddots & \ddots & \vdots \\ \vdots & \cdots & z_1 & z_2 & z_3 & & \\ \vdots & \cdots & & z_1 & z_2 & z_3 & \\ 0 & \cdots & & & 0 & 0 & 0 \end{bmatrix},$$

$$
\begin{aligned}
u_1 &= \alpha_0 a_1 - \theta v_1(r)b_1 + \theta v_2(r)c_1, \\
u_2 &= \alpha_0 a_2 + \theta v_1(r)b_2 + \theta v_2(r)c_2, \\
u_3 &= \alpha_0 a_1 + \theta v_1(r)b_1 + \theta v_2(r)c_1, \\
z_1 &= (1-\theta)(-v_1(r)b_1 + v_2(r)c_1), \\
z_2 &= (1-\theta)(v_1(r)b_2 + v_2(r)c_2), \\
z_3 &= (1-\theta)(v_1(r)b_1 + v_2(r)c_1),
\end{aligned}
$$

$$B = \begin{bmatrix} 0 & 0 & 0 & & & \cdots & 0 \\ a_1 & a_2 & a_1 & & & \cdots & 0 \\ & a_1 & a_2 & a_1 & & & \vdots \\ & & & \ddots & \ddots & \ddots & \\ 0 & \cdots & & a_1 & a_2 & a_1 & \\ 0 & \cdots & & & a_1 & a_2 & a_1 \\ 0 & \cdots & \cdots & & 0 & 0 & 0 \end{bmatrix}, \quad S^{n+1} = \begin{bmatrix} S_{-1}^{n+1} \\ S_0^{n+1} \\ S_1^{n+1} \\ \vdots \\ S_{N-1}^{n+1} \\ S_N^{n+1} \\ S_{N+1}^{n+1} \end{bmatrix},$$

$$G = \left[\varphi_2^{n+1}, g_0^{n+1}, g_1^{n+1}, \cdots, g_{N-1}^{n+1}, g_N^{n+1}, \varphi_3^{n+1}\right]^T.$$

Therefore, we attain $(N+3)\times(N+3)$ order system of linear equations that can be uniquely solved. To initiate the iteration, the initial state vector $S^0 = (S_{-1}^0, S_0^0, S_1^0, \cdots, S_{N+1}^0)^T$, can be evaluated from the initial and end conditions

$$\begin{cases} (P_r)_j^0 = \varphi_1'(r_j), & j = 0,\ N, \\ (P)_j^0 = \varphi_1(r_j), & j = 0, 1, \cdots, N. \end{cases} \qquad (17)$$

Hence, we secure order $(N+3)\times(N+3)$ system of linear equations and can be represented in a matrix frame, thus:

$$A^*S^0 = B^*, \qquad (18)$$

$$\begin{bmatrix} -b_1 & b_2 & b_1 & & \cdots & \cdots & 0 \\ a_1 & a_2 & a_1 & & \cdots & \cdots & 0 \\ 0 & a_1 & a_2 & a_1 & \ldots & \cdots & 0 \\ \vdots & & & & \ddots & \ddots & \vdots \\ \vdots & \cdots & & a_1 & a_2 & a_1 & 0 \\ 0 & \cdots & \cdots & & a_1 & a_2 & a_1 \\ 0 & \cdots & \cdots & & b_1 & b_2 & b_1 \end{bmatrix} \begin{bmatrix} S_{-1}^0 \\ S_0^0 \\ S_1^0 \\ \vdots \\ S_{N-1}^0 \\ S_N^0 \\ S_{N+1} \end{bmatrix} = \begin{bmatrix} \varphi_1'(r_0) \\ \varphi_1(r_0) \\ \varphi_1(r_1) \\ \vdots \\ \varphi_1(r_{N-1}) \\ \varphi_1(r_N) \\ \varphi_1'(r_N) \end{bmatrix}.$$

Subsequently, all numerical experiments are accomplished in Wolfram Mathematica 14.1 with HP Laptop (i7-7500 CPU 2.70GHz, 16.00 GB RAM).

4. Stability analysis

The von Neumann stability is adopted to analyze the stability of the propounded technique for solving the TFCDRE. Presume δ_j^n represents the Fourier growth factor and $\tilde{\delta}_j^n$ its estimation value. Then the error

$$\Theta_j^n = \delta_j^n - \tilde{\delta}_j^n, \qquad n = 0, 1, \cdots, M;\ \ j = 1, 2, \cdots, N-1, \qquad (19)$$

where $\Theta^n = [\delta_1^n, \delta_2^n, \cdots, \delta_{N-1}^n]^T$. For simplicity, we shall consider the stability analysis of the propounded scheme for a

Table 4. Error norms for Example 1 with $T = 0.5$, $\triangle t = 0.002$.

α	N	β	Method in [14]		Proposed Method		Order
			L_2	L_∞	L_2	L_∞	
	4	0.00018	3.1665E-04	4.2478E-04	4.8572E-05	3.3461E-04	$\cdots$
	8	0.000021	2.0867E-05	2.7838E-05	6.6667E-06	3.2394E-06	2.6071
0.25	16	0.0000072	1.3219E-06	1.7842E-06	5.6616E-07	5.6616E-07	2.5165
	32	0.0000357	8.3002E-08	1.1197E-07	4.4315E-07	1.3053E-07	2.1168

Table 5. A comparison of the exact solutions, approximate solutions, and error norms for Example 1 when $\alpha = 0.25$, $\triangle t = 0.001$, $\beta = 0.000055$ and $T = 1$.

r	Exact	$N = 120$	$N = 80$	$N = 40$	$N = 20$
0.1	0.38	0.37999461	0.37999461	0.37999461	0.37999461
0.2	0.72	0.71998987	0.71998987	0.71998987	0.71998988
0.3	1.02	1.01998594	1.01998594	1.01998595	1.01998595
0.4	1.28	1.27998303	1.27998303	1.27998303	1.27998304
0.5	1.50	1.49998138	1.49998139	1.49998139	1.49998139
0.6	1.68	1.67998128	1.67998128	1.67998128	1.67998129
0.7	1.82	1.81998297	1.81998297	1.81998297	1.81998299
0.8	1.92	1.91998665	1.91998665	1.91998665	1.91998667
0.9	1.98	1.97999238	1.97999238	1.97999238	1.97999239
L_∞		1.88833E-05	1.88803E-05	1.88752E-05	1.88618E-05
L_2		1.48629E-04	1.21351E-04	8.57927E-05	1.88618E-05

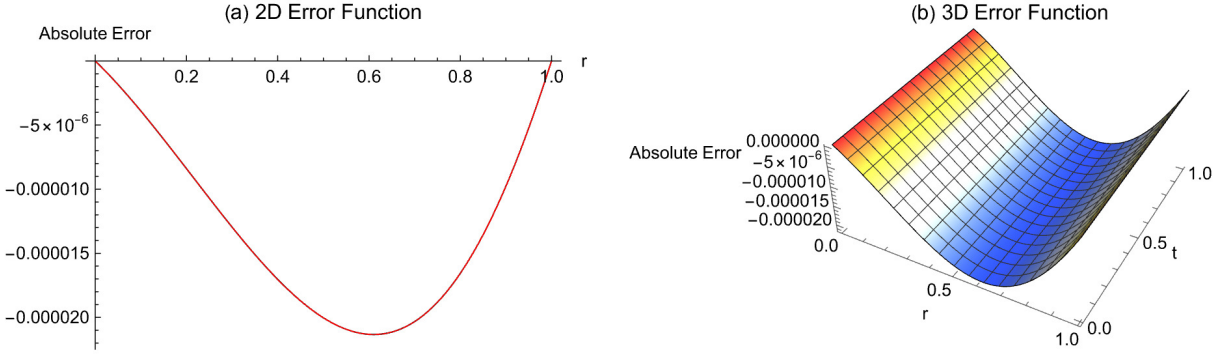

Figure 2. 2D and 3D error plot of Example 1 at $N = 100$, $\alpha = 0.25$, $\triangle t = 0.01$ and $T = 1$.

force-free case ($g = 0$). Employing Eq. (12) and Eq. (19), we attain the error equation as

$$\begin{aligned}
&(\alpha_0 a_1 - \theta v_1(r) b_1 - \theta v_2(r) c_1 + \theta v_3(r) a_1)\Theta_{j-1}^{j+1} \\
&+ (\alpha_0 a_2 - \theta v_2(r) c_2 + \theta v_3(r))\Theta_j^{n+1} + (\alpha_0 a_1 + \theta v_1(r) b_1 - \theta v_2(r) c_1 \\
&+ \theta v_3(r) a_1)\Theta_{j+1}^{n+1} = \alpha_0 z_n (a_1 \Theta_{j-1}^0 + a_2 \Theta_j^0 + a_1 \Theta_{j+1}^0) \\
&+ \alpha_0 \sum_{l=0}^{n-1} (w_l - w_{l+1})[a_1 \Theta_{j-1}^{n-l} + a_2 \Theta_j^{n-l} + a_1 \Theta_{j+1}^{n-l}] \\
&- (1-\theta) v_1(r)(-b_1 \Theta_{j-1}^n + b_1 \Theta_{j+1}^n) + (1-\theta) v_2(r)(c_1 \Theta_{j-1}^n \\
&+ c_2 \Theta_j^n + c_1 \Theta_{j+1}^n) - (1-\theta) v_3(r)(a_1 \Theta_{j-1}^n + a_2 \Theta_j^n + a_1 \Theta_{j+1}^n).
\end{aligned} \tag{20}$$

Now, we can write the initial and boundary conditions as

$$\Theta_j^0 = \varphi_1(r_j), \quad j = 1:1:N, \tag{21}$$

and

$$\Theta_0^n = \varphi_2(t_n), \quad \Theta_N^n = \varphi_3(t_n), \quad n = 0:1:M. \tag{22}$$

Define the mesh function as:

$$\Theta^n = \begin{cases} \Theta_j^n, & r_j - \dfrac{h}{2} < r \le r_j + \dfrac{h}{2}, \quad j = 1, 2, \cdots, N-1 \\ 0, , & a \le r \le a + \dfrac{h}{2}, \text{ or } b - \dfrac{h}{2} \le r \le b. \end{cases} \tag{23}$$

The Fourier series expansion for $\Theta^n(r)$ can be designated as:

$$\Theta^n(r) = \sum_{m=-\infty}^{\infty} \Psi^n(m) e^{\frac{i2\pi mr}{(b-a)}}, \quad n = 0:1:M, \tag{24}$$

where

$$\Psi^n(m) = \frac{1}{(b-a)} \int_a^b \Theta^n(r) e^{\frac{-i2\pi mr}{(b-a)}} dr, \tag{25}$$

and

$$\Theta^n = [\Theta_1^n, \Theta_2^n, \cdots, \Theta_{N-1}^n]^T. \tag{26}$$

Using the norm $\|\cdot\|_2$, we secure

$$\begin{aligned}\|\Theta^n\|_2 &= \left(\sum_{i=1}^{N-1} h|\Theta_i^n|^2\right)^{\frac{1}{2}} \\ &= \left(\int_a^{a+\frac{h}{2}} |\Theta^n|^2 dr + \sum_{i=1}^{N-1}\int_{r_i-\frac{h}{2}}^{r_i+\frac{h}{2}} |\Theta^n|^2 dr + \int_{b-\frac{h}{2}}^{b} |\Theta^n|^2 dr\right)^{\frac{1}{2}}. \\ &= \left(\int_a^b |\Theta^n|^2 dr\right)^{\frac{1}{2}}.\end{aligned}$$

Applying Parseval's identity (6), we obtain

$$\int_a^b |\Theta^n(r)|^2 dr = \sum_{m=-\infty}^{\infty} |\Psi^n(m)|^2.$$

Thus, we gain

$$\|\Theta^n\|_2^2 = \sum_{m=-\infty}^{\infty} |\Psi^n(m)|^2. \tag{27}$$

Suppose Eqs. (20) - (22) have solution in Fourier series form as:

$$\Theta_j^n = \Psi^n e^{i\alpha h j}, \tag{28}$$

where $\alpha = 2\pi m \div b - a$, $i = \sqrt{-1}$, h, Ψ, α are the Fourier coefficient, the mode number, and the element size respectively. Employing Eq. (28) in Eq. (20), we secure

$$\begin{aligned}&(\alpha_0 a_1 - \theta v_1(r) b_1 - \theta v_2(r) c_1 + \theta v_3(r) a_1)\Psi^{n+1} e^{i\alpha h(j-1)} \\ &+ (\alpha_0 a_2 - \theta v_2(r) c_2 + \theta v_3(r) a_2)\Psi^{n+1} e^{i\alpha h j} + (\alpha_0 a_1 + \theta v_1(r) b_1 \\ &- \theta v_2(r) c_1 + \theta v_3(r) a_1)\Psi^{n+1} e^{i\alpha h(j+1)} = \alpha_0 z_n [a_1 e^{i\alpha h(j-1)} \\ &+ a_2 e^{i\alpha h j} + a_1 e^{i\alpha h(j+1)}]\Psi^0 + \alpha_0 \sum_{l=0}^{n-1}(w_l - w_{l+1})[a_1 e^{i\alpha h(j-1)} \\ &+ a_2 e^{i\alpha h j} + a_1 e^{i\alpha h(j+1)}]\Psi^{n-l} - (1-\theta) v_1(r)[-b_1 e^{i\alpha h(j-1)} \\ &+ b_1 e^{i\alpha h(j+1)}]\Psi^n + (1-\theta) v_2(r)[c_1 e^{i\alpha h(j-1)} + c_2 e^{i\alpha h j} \\ &+ c_1 e^{i\alpha h(j+1)}]\Psi^n - (1-\theta) v_3(r)[a_1 e^{i\alpha h(j-1)} + a_2 e^{i\alpha h j} \\ &+ a_1 e^{i\alpha h(j+1)}]\Psi^n.\end{aligned}$$

Dividing throughout by $e^{i\alpha h}$, employing the expression $e^{i\alpha h} + e^{-i\alpha h} = 2\cos(\alpha h)$ and rearranging the terms, we secure

$$\begin{aligned}&[(2\alpha_0 a_1 - 2\theta v_2(r) c_1 + 2\theta v_3(r) a_1)cos(\alpha h) + \alpha_0 a_2 - \theta v_2(r) c_2 \\ &+ \theta v_3(r) a_2 + (2i\theta v_1(r) b_1) sin(\alpha h)]\Psi^{n+1} = \alpha_0 w_n [a_2 \\ &+ 2a_1 cos(\alpha h)]\Psi^0 - (1-\theta)[2iv_1(r) b_1 sin(\alpha h) \\ &- v_2(r)(c_2 + 2c_1 cos(\alpha h)) + v_3(r)(a_2 + 2a_1 cos(\alpha h))]\Psi^n \\ &+ \alpha_0(a_2 + 2a_1 cos(\alpha h)) \sum_{l=0}^{n-1}(w_l - w_{l+1})\Psi^{n-l}.\end{aligned}$$

Next, applying the relation $cos(\alpha h) = 1 - 2sin^2(\alpha h \div 2)$, substituting the values of a_1, a_2, b_1, c_1 and c_2 in the above equation, and simplifying further, we gain

$$\Psi^{n+1} = \frac{z_n \alpha_0}{Q}\Psi^0 - \frac{Q_1}{Q}\Psi^n + \frac{\alpha_0}{Q}\sum_{l=0}^{n-1}(w_l - w_{l+1})\eta^{n-l}, \tag{29}$$

where

$$\begin{aligned}Q_1 &= \frac{(1-\theta)[12v_2(r)(2+\beta)sin^2(\frac{\alpha h}{2}) + 6hv_1(r)sin(\alpha h)]}{(6-(4-\beta)sin^2(\frac{\alpha h}{2}))h^2} \\ &+ \frac{(1-\theta)[h^2 v_3(r)(6-(4-\beta)sin^2(\frac{\alpha h}{2}))]}{(6-(4-\beta)sin^2(\frac{\alpha h}{2}))h^2},\end{aligned}$$

$$\begin{aligned}Q &= (\alpha_0 + \theta v_3(r)) \\ &+ \frac{12\theta v_2(r)(2+\beta)sin^2 - 6\theta i h v_1(r) sin(\alpha h) + (\frac{\alpha h}{2})}{h^2(6-(4-\beta)sin^2(\frac{\alpha h}{2}))}.\end{aligned}$$

Given any complex number, $q_1 + iq_2 \geq q_3 + iq_4$, provided that $q_1 \geq q_3$ or $q_2 \geq q_4$ [49]. Obviously, $Q \geq 1$ and $Q_1 > 0$ for $\beta > -2$.

4.1. proposition

Suppose that Ψ^n is a solution of Eq. (29), then we attain

$$|\Psi^n| \leq |\Psi^0|, \quad n = 0(1)M. \tag{30}$$

Proof

Mathematical induction is utilized to certify the inequality, equation (30). For $n = 0$, system (29) emerges as

$$\begin{aligned}\Psi^1 &= \frac{w_0\alpha_0}{Q}\Psi^0 - \frac{Q_1}{Q}\Psi^0 \leq \frac{w_0\alpha_0}{Q}\Psi^0, \\ \Psi^1 &\leq \Psi^0, \quad Q \geq 1, \\ |\Psi^{n+1}| &\leq |\Psi^0|.\end{aligned}$$

Suppose that $n = 0, 1, 2, \cdots, N-1$, $|\Psi^n| \leq |\Psi^0|$ is true, from Eq. (29), we secure

$$\begin{aligned}\Psi^{n+1} &= \frac{w_n\alpha_0}{Q}\Psi^0 - \frac{Q_1}{Q}\Psi^n + \frac{\alpha_0}{Q}\sum_{l=0}^{n-1}(w_l - w_{l+1})\Psi^{n-l} \\ |\Psi^{n+1}| &\leq \frac{w_n\alpha_0}{Q}|\Psi^0| + \frac{\alpha_0}{Q}\sum_{l=0}^{n-1}(w_l - w_{l+1})|\Psi^{n-l}| \\ &\leq \frac{w_n\alpha_0}{Q}|\Psi^0| + \frac{\alpha_0}{Q}\sum_{l=0}^{n-1}(w_l - w_{l+1})|\Psi^0| \\ &\leq \frac{1}{Q}\left[\sum_{l=0}^{n-1}(w_l - w_{l+1}) + w_n\right]|\Psi^0| \\ &= \frac{1}{Q}[(1-w_1) + (w_1 - w_2) + \cdots + (w_{n-1} - w_n) + w_n]|\Psi^0| \\ |\Psi^{n+1}| &= \frac{1}{q}\Psi^0 \leq |\Psi^0|.\end{aligned}$$

Certainly, $|\Psi^{n+1}| \leq |\Psi^0|$, so that $\|\Psi^{n+1}\|_2 \leq \|\Psi^0\|_2$. This signifies that the suggested approach is unconditionally stable.

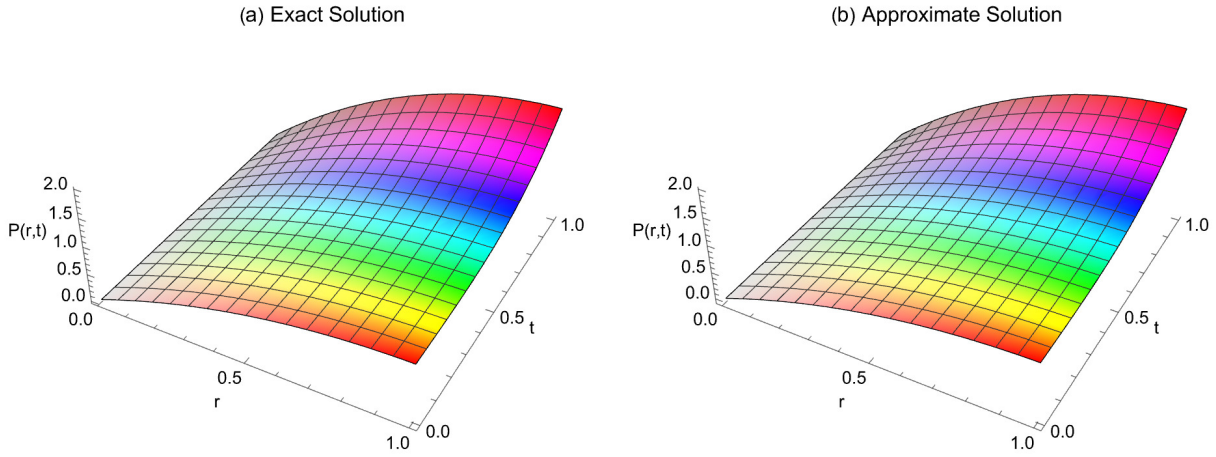

Figure 3. A 3D comparison between the exact solutions and approximate solutions with $T = 1$, $\alpha = 0.35$, $\triangle t = 0.01$ and $N = 80$ for Example 1.

5. Convergence analysis

We adopted the procedure engaged by Kadalbajoo and Arora [50] in addressing the convergence analysis. Firstly, we present the following theorems and lemma [51, 52].

5.1. Theorem [51, 52]

Presume that $p(r,t) \in C^4[a,b]$, $f \in C^2[a,b]$ and $\Theta = \{a = r_0, r_1, \cdots, r_n = b\}$ be the equally spaced partitioning of $[a,b]$ of length h such that $r_j = a + jh$, $j = 0(1)N$. Assume $\hat{P}(r,t)$ is the unique spline interpolating the solution of equation (1) at the spatial grid point $r_j \in \Phi$, $j = 0(1)N$, then there exists a constant W_j from h, so that $\forall t \geq 0$, we secure

$$\|D^j(p(r,t) - \hat{P}(r,t))\|_\infty \leq W_j h^{4-j}, \quad j = 0, 1, 2. \tag{31}$$

5.2. Lemma [31]

The ExCBS set $\{B_{-1}, B_0, \cdots, B_{N+1}\}$ expressed in definition, equation (7) fulfills the inequality bellow

$$\sum_{j=-1}^{N+1} |B_j(r,\beta)| \leq 1.75, \quad 0 \leq r \leq 1. \tag{32}$$

5.3. Theorem

If $P(r,t)$ be the numerical approximate solution to the exact solution $p(r,t)$ of the TFCDRE, Eqs. (1)–(3). Further, assume $f \in C^2[0,1]$, we achieve

$$\|p(r,t) - P(r,t)\|_\infty \leq Wh^2, \quad \forall\, t \geq 0, \tag{33}$$

where h is adequately small and $W > 0$ is independent of h.

Proof:

We presume that $\hat{P}(r,t) = \sum_{j=-1}^{N+1} e_j^n(t) B_j(r,\beta)$ be the computed spline approximation for $P(r,t)$. By the concept of triangular inequality, we arrive at the following

$$\|p(r,t) - P(r,t)\|_\infty \leq \|p(r,t) - \hat{P}(r,t)\|_\infty + \|\hat{P}(r,t)\| - P(r,t)\|_\infty. \tag{34}$$

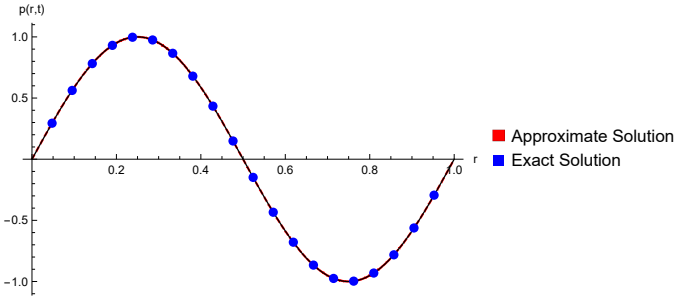

Figure 4. Exact and approximate solutions for $N = 100$, $\alpha = 0.5$, and $T = 1$ for Example 2.

By Theorem (5.1), we secure

$$\|D^j(p(r,t)) - \hat{P}(r,t))\|_\infty \leq W_j h^{4-j}, \quad j = 0, 1, 2. \tag{35}$$

Using the inequality (35), we achieve

$$\|p(r,t) - P(r,t)\|_\infty \leq W_0 h^4 + \|\hat{P}(r,t)\| - P(r,t)\|_\infty. \tag{36}$$

The collocation conditions are

$$Lp(r_j,t) = LP(r_j,t) = g(r_j,t), \quad j = 0, 1, 2, \cdots, N.$$

Presume

$$L\hat{P}(r_j,t) = \hat{g}(r_j,t), \quad j = 0, 1, 2, \cdots, N.$$

Thus, the difference equations $L(\hat{P}(r_j,t) - P(r_j,t))$ of the given problem at any time level n, can be written as

$$\begin{aligned}
&([\alpha_0 + \theta v_3(r)]a_1 - \theta v_1(r)b_1 - \theta v_2(r)c_1)\Upsilon_{j-1}^{n+1} \\
&\quad + ([\alpha_0 + \theta v_3(r)]a_2 - \theta v_2(r)c_2)\Upsilon_j^{n+1} \\
&\quad + ([\alpha_0 + \theta v_3(r)]a_1 + \theta v_1(r)b_1 - \theta v_2(r)c_1)\Upsilon_{j+1}^{n+1} \\
&= \alpha_0(a_1\Upsilon_{j-1}^n + a_2\Upsilon_j^n + a_1\Upsilon_{j+1}^n) - \alpha_0 \sum_{l=1}^{n} w_l\{a_1[\Upsilon_{j-1}^{n+1-l} - \Upsilon_{j-1}^{n-l}] \\
&\quad + a_2[\Upsilon_j^{n+1-l} - \Upsilon_j^{n-l}] + a_1[\Upsilon_{j+1}^{n+1-l} - \Upsilon_{j+1}^{n-l}]\}
\end{aligned}$$

Table 6. Error norms of Example 2 for $\beta = 0.000121$, $\triangle t = 0.002$, $T = 1$.

α	N	Method in Ref. [16]		Proposed Method		
		L_2	L_∞	L_2	Order	CPU
0.4	4	4.62E-01	1.8718E-01	2.4139E-01	$\cdots$	3.1557
	8	2.38E-01	5.1871E-02	9.4717E-02	1.8515	3.8014
	16	1.22E-01	1.3297E-02	3.4333E-02	1.9639	4.8263
	32	6.20E-02	3.4119E-03	1.2371E-02	1.9624	11.1952
	64	3.13E-02	9.0175E-04	4.6204E-03	1.9198	27.9197
	128	1.57E-02	2.7274E-04	1.9749E-03	1.7252	132.387
0.6	4	4.55E-01	1.8599E-01	2.4023E-01	$\cdots$	4.8521
	8	2.34E-01	5.1502E-02	9.4201E-02	1.8525	5.3389
	16	1.20E-01	1.3198E-02	3.4136E-02	1.9643	8.0766
	32	6.08E-02	3.3839E-03	1.2294E-02	1.9635	14.2045
	64	3.07E-02	8.9297E-04	4.5839E-03	1.9219	52.9798
	128	1.54E-02	2.6864E-04	1.9492E-03	1.7329	101.573
0.8	4	4.48E-01	1.8477E-01	2.3906E-01	$\cdots$	5.1352
	8	2.30E-01	5.1121E-02	9.3675E-02	1.8537	5.6101
	16	1.18E-01	1.3090E-02	3.3920E-02	1.9654	7.8377
	32	5.97E-02	3.3479E-03	1.2190E-02	1.9671	15.0552
	64	3.01E-02	8.7654E-04	4.5093E-03	1.9334	35.7541
	128	1.51E-02	2.5695E-04	1.8693E-03	1.7703	177.832

Table 7. Error norms with $\beta = 0.000058$ and various α values of Example 2.

t	L_2		L_∞	
	$\alpha = 0.2, N = 70$ $\triangle t = 0.002$	$\alpha = 0.7, N = 50$ $\triangle t = 0.001$	$\alpha = 0.2, N = 70$ $\triangle t = 0.002$	$\alpha = 0.7, N = 50$ $\triangle t = 0.001$
0.2	1.55457E-04	2.21035E-04	2.89783E-05	4.73955E-05
0.4	6.26458E-04	9.60310E-04	1.16971E-04	2.08712E-04
0.6	1.41414E-03	2.21785E-03	2.64279E-04	4.85075E-04
0.8	2.51921E-03	3.99636E-03	4.71075E-04	8.77271E-04
1.0	3.94212E-03	6.29728E-03	7.37473E-04	1.38574E-03

Table 8. Approximate solutions with $\alpha = 0.65$, $T = 1$ for Example 2.

r	Exact	Approximate Solution		Absolute Error	
		$N = 60$	$N = 100$	$N = 60$	$N = 100$
0.1	0.58778853	0.58778525	0.58757200	0.00053630814	0.00021325027
0.2	0.95105652	0.95014031	0.95069221	0.00091620970	0.00036430573
0.3	0.95105652	0.95006546	0.95066246	0.00099105915	0.00039405901
0.4	0.58778525	0.58705561	0.58749515	0.00072964371	0.00029010005
0.5	0.00000000	-0.00023013	-0.00009147	0.00023013212	0.00009146689
0.6	-0.58778525	-0.58746788	-0.58765901	0.00031736832	0.00012624398
0.7	-0.95105652	-0.95035318	-0.95077680	0.00070334003	0.00027971858
0.8	-0.95105652	-0.95027776	-0.95074682	0.00077875972	0.00030969909
0.9	-0.58778525	-0.58727340	-0.58758170	0.00051185126	0.00020355098

$$- (1-\theta)v_1(r)(-b_1\Upsilon^n_{j-1} + b_1\Upsilon^n_{j+1}) + (1-\theta)v_2(r)(c_1\Upsilon^n_{j-1} + c_2\Upsilon^n_j + c_1\Upsilon^n_{j+1}) - (1-\theta)v_3(r)(a_1\Upsilon^n_{j-1} + a_2\Upsilon^n_j + a_1\Upsilon^n_{j+1}) + g^{n+1}_j. \quad (37)$$

The boundary conditions can take the form:

$$a_1\Upsilon^{n+1}_{j-1} + a_2\Upsilon^{n+1}_j + a_1\Upsilon^{n+1}_{j+1} = 0, \quad j = 0, N,$$

where

$$\Upsilon^n_j = D^n_j - d^n_j, \quad j = -1, 0, 1, \cdots, N+1, \quad (38)$$

and

$$X^n_j = h^2[g^n_j - \hat{g}^n_j], \quad j = 0:1:N.$$

From inequality (35), we secure

$$|X^n_j| = h^2|g^n_j - \hat{g}^n_j| \leq Wh^4, \quad j =, 0, 1, \cdots, N. \quad (39)$$

Table 9. Absolute errors at different time levels for $\alpha = 0.35$, $\triangle t = 0.002$, $T = 1$.

r	Time					
	T=1.0	T=0.9	T=0.7	T=0.5	T=0.3	T=0.1
0.1	1.9605E-04	1.5852E-04	9.5456E-05	4.8341E-05	1.7123E-05	1.7089E-06
0.2	3.3511E-04	2.7094E-04	1.6312E-04	8.2582E-05	2.9238E-05	2.9137E-06
0.3	3.6290E-04	2.9337E-04	1.7655E-04	8.9325E-05	3.1592E-05	3.1387E-06
0.4	2.6797E-04	2.1653E-04	1.3017E-04	6.5759E-05	2.3194E-05	2.2864E-06
0.5	8.6021E-05	6.9337E-05	4.1421E-05	2.0732E-05	7.1946E-06	6.7512E-07
0.6	1.1367E-04	9.2182E-05	5.5917E-05	2.8619E-05	1.0321E-05	1.0826E-06
0.7	2.5470E-04	2.0622E-04	1.2459E-04	6.3407E-05	2.2647E-05	2.3138E-06
0.8	2.8268E-04	2.2880E-04	1.3812E-04	7.0959E-05	2.5021E-05	2.5412E-06
0.9	1.8596E-04	1.5049E-04	9.0822E-05	4.6139E-05	1.6432E-05	1.6651E-06

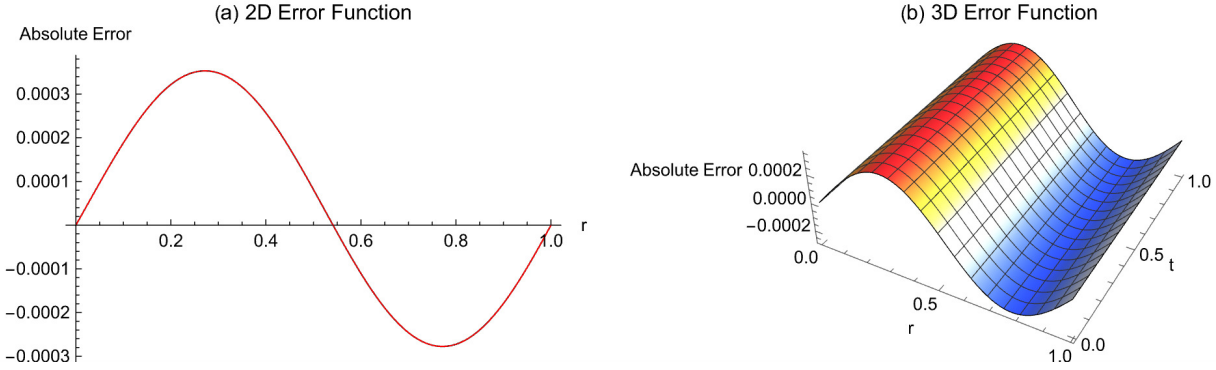

Figure 5. 2D and 3D error plot of Example 2 at $\alpha = 0.50$, $N = 100$, $T = 1$.

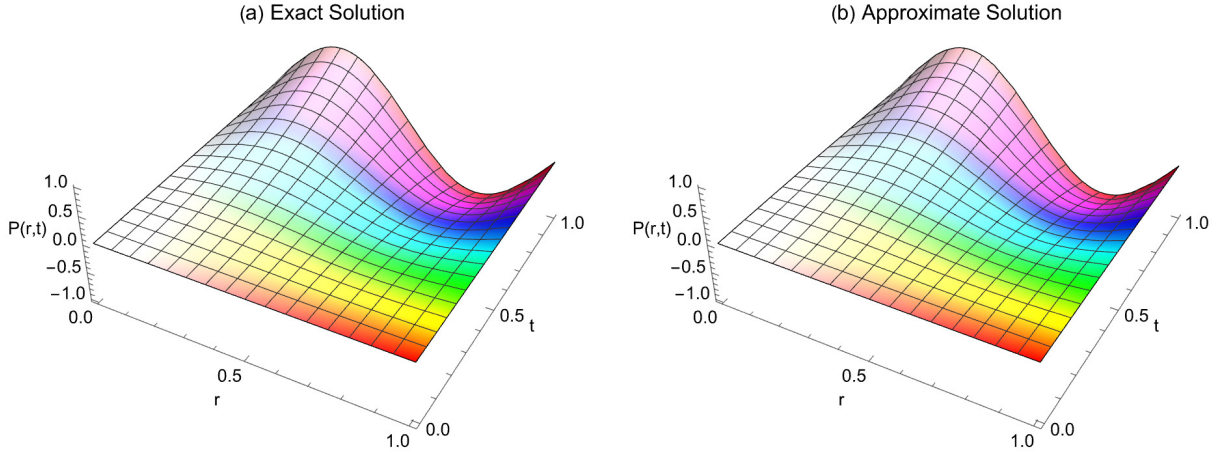

Figure 6. A 3D plot of the exact and approximate solutions for $\alpha = 0.25$, $T = 1$, and $r \in [0, 1]$ for Example 2.

We define $X^n = max\{|X_j^n|;\ 0 \le j \le N\}$, $\hat{\mu}_j^n = |\Upsilon_j^n|$ and $\hat{\mu}^n = max\{|\hat{\mu}_j^n|,\ 0 \le i \le N\}$. For $n = 0$, then Eq. (37) transforms into the following

$$\begin{aligned}
&([\alpha_0 + \theta v_3(r)]a_1 - \theta v_1(r)b_1 - \theta v_2(r)c_1)\Upsilon_{j-1}^1 \\
&\quad + ([\alpha_0 + \theta v_3(r)]a_2 - \theta v_2(r)c_2)\Upsilon_j^1 \\
&\quad + ([\alpha_0 + \theta v_3(r)]a_1 + \theta v_1(r)b_1 - \theta v_2(r)c_1)\Upsilon_{j+1}^1 \\
&= \alpha_0(a_1\Upsilon_{j-1}^0 + a_2\Upsilon_j^0 + a_1\Upsilon_{j+1}^0) - (1-\theta)[(-v_1(r)b_1 - v_2(r)c_1 \\
&\quad + v_3(r)a_1)\Upsilon_{j-1}^0 + (v_2(r)c_2 + v_3(r)a_2)\Upsilon_j^0 \\
&\quad + (v_1(r)b_1 - v_1(r)c_1 + v_3(r)a_1)\Upsilon_{j+1}^0] + \frac{1}{h^2}X_j^1, \quad j = 0(1)N.
\end{aligned}$$

Engaging the initial condition, $\mu^0 = 0$:

$$\begin{aligned}
&([\alpha_0 + \theta v_3(r)]a_2 - \theta v_2(r)c_2)\Upsilon_j^1 = -((\alpha_0 + v_3(r))a_1 \\
&- \theta v_2(r)c_1)(\Upsilon_{j-1}^1 + \Upsilon_{j+1}^1) + \theta v_1(r)b_1(\Upsilon_{j-1}^1 - \Upsilon_{j+1}^1) + \frac{1}{h^2}X_j^1.
\end{aligned}$$

Table 10. A comparison of approximate solutions for Example 3.

α	r	$N = 160$	$N = 80$	$N = 40$	$N = 20$	Exact
	0.1	1.1753909	1.1749576	1.1732263	1.1663297	1.175571
	0.2	1.9018059	1.9010650	1.8981048	1.8863131	1.902113
	0.3	1.9017801	1.9009772	1.8977691	1.8849906	1.902113
	0.4	1.1753240	1.1747301	1.1723568	1.1629046	1.175571
0.25	0.5	-0.0000803	-0.0002731	-0.0010431	-0.0041090	0.000000
	0.6	-1.1754682	-1.1752203	-1.1742295	-1.1702807	-1.175571
	0.7	-1.9018815	-1.9013220	-1.8990862	-1.8901781	-1.902113
	0.8	-1.9018556	-1.9012337	-1.8987485	-1.8888476	-1.902113
	0.9	-1.1754010	-1.1749917	-1.1733559	-1.1668392	-1.175571
	0.1	1.1754092	1.1749788	1.1732589	1.1664072	1.175571
	0.2	1.9018373	1.9011016	1.8981618	1.8864507	1.902113
	0.3	1.9018143	1.9010176	1.8978339	1.8851518	1.902113
	0.4	1.1753497	1.1747613	1.1724104	1.1630465	1.175571
0.50	0.5	-0.0000714	-0.0002603	-0.0010150	-0.0040200	0.000000
	0.6	-1.1754778	-1.1752283	-1.1742312	-1.1702575	-1.175571
	0.7	-1.9019043	-1.9013452	-1.8991109	-1.8902089	-1.902113
	0.8	-1.9018812	-1.9012606	-1.8987808	-1.8889014	-1.902113
	0.9	-1.1754179	-1.1750097	-1.1733784	-1.1668794	-1.175571
	0.1	1.1754848	1.1750582	1.1733535	1.1665621	1.175571
	0.2	1.9019666	1.9012377	1.8983252	1.9832536	1.902113
	0.3	1.9019547	1.9011662	1.8980151	1.8854625	1.902113
	0.4	1.1754541	1.1748732	1.1725523	1.1633070	1.175571
0.75	0.5	-0.0000365	-0.0002202	-0.0009543	-0.0038776	0.000000
	0.6	-1.1755194	-1.1752678	-1.1742623	-1.1702551	-1.175571
	0.7	-1.9020002	-1.9014416	-1.8992094	-1.8903153	-1.902113
	0.8	-1.9019882	-1.9013695	-1.8988970	-1.8890460	-1.902113
	0.9	-1.1754885	-1.1750818	-1.1734564	-1.1669810	-1.175571

Table 11. A comparison of error norms of Example 3 for $T = 1$, $\triangle t = 0.004$.

α	N	L_∞	L_2	Order	CPU
	10	6.70327E-02	1.37377E-01	$\cdots$	1.099545
	20	1.70832E-02	4.92581E-02	1.972287	3.100442
0.4	40	4.33116E-03	1.75113E-02	1.979753	4.457339
	80	1.09336E-03	6.25102E-03	1.985985	22.06897
	160	2.83073E-04	2.28800E-03	1.949522	109.9835
	10	6.65458E-02	1.36639E-01	$\cdots$	1.511608
	20	1.69526E-02	4.89559E-02	1.972841	1.760997
0.6	40	4.28591E-03	1.73580E-02	1.983833	5.425586
	80	1.07072E-03	6.13206E-03	2.001020	22.18238
	160	2.66098E-04	2.15448E-03	2.313169	89.75226
	10	6.59027E-02	1.35646E-01	$\cdots$	1.258734
	20	1.67498E-02	4.84648E-02	1.976194	2.255291
0.8	40	4.18826E-03	1.70006E-02	1.999721	6.126450
	80	1.00102E-03	5.74717E-03	2.064880	14.56493
	160	2.03423E-04	1.65290E-03	2.298916	95.96395

Taking norms of Υ_j^n and X_j^n with sufficiently small h, we attain

$$\hat{\mu}_j^1 \leq \frac{6Wh^4}{(\alpha_0 + v_3(r))h^2(2+\beta) + 12\theta v_2(r)(2+\beta) - 6\theta v_1(r)h}, \quad j = 0:1:N.$$

and employing the end conditions, we conclude that

$$\hat{\mu}^1 \leq W_1 h^2, \tag{40}$$

where W_1 is independent of h. Utilizing mathematical induction on n, we assume that $\hat{\mu}_j^k \leq W_k h^2$ is true for $k = 1, 2, \cdots n$, and $W = max\{W_k : 0 \leq k \leq n\}$, then Eq. (37) take the form as

Table 12. A comparison of maximum absolute error for $T = 1$, $N = 100$, $\triangle t = 0.004$ of Example 3.

r	$\alpha = 0.9$	$\alpha = 0.7$	$\alpha = 0.5$	$\alpha = 0.3$	$\alpha = 0.1$
0.1	0.000326947	0.000395067	0.000413889	0.000420386	0.000423292
0.2	0.000558258	0.000675049	0.000707479	0.000718778	0.000723875
0.3	0.000603194	0.000730501	0.000766227	0.000778916	0.000784743
0.4	0.000442829	0.000538391	0.000565909	0.000576129	0.000581009
0.5	0.000137288	0.000170909	0.000181892	0.000186783	0.000189440
0.6	0.000197183	0.000232066	0.000239612	0.000240856	0.000240830
0.7	0.000432565	0.000516335	0.000537336	0.000543189	0.000545208
0.8	0.000477883	0.000572190	0.000596472	0.000603698	0.000606433
0.9	0.000313833	0.000376200	0.000392413	0.000397345	0.000399266
L_∞	6.11999E-04	7.40726E-04	7.76705E-04	7.89390E-04	7.95176E-04
L_2	3.93726E-03	4.74750E-03	4.96810E-03	5.04213E-03	5.07434E-03

$$
\begin{aligned}
&([\alpha_0+\theta v_3(r)]a_1-\theta v_1(r)b_1-\theta v_2(r)c_1)\Upsilon_{j-1}^{n+1}\\
&\quad+([\alpha_0+\theta v_3(r)]a_2-\theta v_2(r)c_2)\Upsilon_j^{n+1}+([\alpha_0+\theta v_3(r)]a_1\\
&+\theta v_1(r)b_1-\theta v_2(r)c_1)\Upsilon_{j+1}^{n+1}=\alpha_0(a_1\Upsilon_{j-1}^{n}+a_2\Upsilon_j^{n}+a_1\Upsilon_{j+1}^{n})\\
&\quad-\alpha_0\sum_{l=1}^{n}z_l\{a_1[\Upsilon_{j-1}^{n+1-l}-\Upsilon_{j-1}^{n-l}]+a_2[\Upsilon_j^{n+1-l}-\Upsilon_j^{n-l}]\\
&+a_1[\Upsilon_{j+1}^{n+1-l}-\Upsilon_{j+1}^{n-l}]\}-(1-\theta)[(-v_1(r)b_1-v_2(r)c_1\\
&\quad+v_3(r)a_1)\Upsilon_{j-1}^{n}+(v_2(r)c_2+v_3(r))\Upsilon_j^{n}\\
&\quad+(v_1(r)b_1-v_2(r)c_1+v_3(r)a_1)\Upsilon_{j+1}^{n}]+\frac{1}{h^2}X_j^{n}.
\end{aligned}
$$

After rearranging the terms, we secure

$$
\begin{aligned}
&([\alpha_0+\theta v_3(r)]a_1-\theta v_1(r)b_1-\theta v_2(r)c_1)\Upsilon_{j-1}^{n+1}\\
&\quad+([\alpha_0+\theta v_3(r)]a_2-\theta v_2(r)c_2)\Upsilon_j^{n+1}+([\alpha_0+\theta v_3(r)]a_1\\
&\quad+\theta v_1(r)b_1-\theta v_2(r)c_1)\Upsilon_{j+1}^{n+1}=\alpha_0[(w_0-w_1)(a_1\Upsilon_{j-1}^{n}\\
&+a_2\Upsilon_j^{n}+a_1\Upsilon_{j+1}^{n})+(w_1-w_2)(a_1\Upsilon_{j-1}^{n-1}+a_2\Upsilon_j^{n-1}+a_1\Upsilon_{j+1}^{n-1})\\
&\quad+\cdots+(w_{n-1}-w_n)(a_1\Upsilon_{j-1}^{1}+a_2\Upsilon_j^{1}+a_1\Upsilon_{j+1}^{1})\\
&+w_n(a_1\Upsilon_{j-1}^{0}+a_2\Upsilon_j^{0}+a_1\Upsilon_{j+1}^{0})]-(1-\theta)[(-v_1(r)b_1v_2(r)c_1\\
&+v_3(r))\Upsilon_{j-1}^{n}+(v_2(r)c_2+v_3(r)a_2)\Upsilon_j^{n}+(v_1(r)b_1-v_2(r)c_1\\
&\quad+v_3(r)a_1)\Upsilon_{j+1}^{n}]+\frac{1}{h^2}X_j^{n+1}.
\end{aligned}
$$

Again taking absolute values of Υ_j^{n+1} and X_j^{n+1}, and secure

$$
\hat{\mu}_j^{n+1}\le\frac{6h^2(\alpha_0\sum_{l=0}^{n-1}(w_l-w_{l+1})Wh^2+Wh^2-(1-\theta)W_nh^2)}{(\alpha_0+v_3(r))h^2(2+\beta)+12\theta v_2(r)(2+\beta)-6\theta v_1(r)h},\tag{41}
$$

from the end conditions

$$
\hat{\mu}_j^{n+1}\le Wh^2,\quad j=-1,\ N+1.
$$

Therefore, for every value of n, we acquire

$$
\hat{\mu}_j^{n+1}\le Wh^2.\tag{42}
$$

Now, from above inequality

$$
\hat{P}(r,t)-P(r,t)=\sum_{j=-1}^{N+1}(d_j(t)-D_j(t))B_j(r,\beta).
$$

Therefore, from the norm, we achieve

$$
\|\hat{P}(r,t)-P(r,t)\|_\infty\le\frac{7}{4}Wh^2.\tag{43}
$$

Employing the triangular inequality (43), we receive

$$
\|p(r,t)-P(r,t)\|_\infty\le\|p(r,t)-\hat{P}(r,t)\|_\infty+\|\hat{P}(r,t)-P(r,t)\|_\infty.\tag{44}
$$

Adopting the inequality (35), (42), and (44), we attain

$$
\|p(r,t)-\hat{P}(r,t)\|_\infty+\|\hat{P}(r,t)-P(r,t)\|_\infty\le W_0h^4+\frac{7}{4}Wh^2=\tilde{W}h^2,
$$

where $\tilde{W}=W_0h^2+\frac{7}{4}W$. Accordingly, there exists a constant $\tilde{W}$ independent of h.

$$
\|p(r,t)-\hat{P}(r,t)\|_\infty\le\tilde{W}h^2.
$$

Applying the preceding theorem and expression (11), it is concluded that the suggested numerical scheme is unconditionally convergent. Thus,

$$
\|p(r,t)-P(r,t)\|_\infty\le\tilde{W}h^2+C_p\Delta t^{2-\alpha},
$$

where $\tilde{W}$ is constant and $\alpha\in(0,1]$. Accordingly, the suggested numerical scheme experimental order of convergence (EOC) is $O(h^2+\Delta t^{2-\alpha})$.

6. Expository examples and discussions

In this section, three numerical experiments were presented to validate the efficacy and simplicity of our method by engaging the error norms $L_\infty(N_j)$, $L_2(N_j)$ and the EOC as

$$
L_\infty(N_j)=\max_{0\le j\le N}|P(r_j,t)-p(r_l,t)|,
$$

$$
L_2(N_j)=\sqrt{h\sum_{j=0}^{N}|P(r_j,t)-p(r_l,t)|^2},
$$

and

$$
Order=log_2\Big(\frac{log(L_\infty(N_j))}{log(L_\infty(N_{j+1}))}\Big).
$$

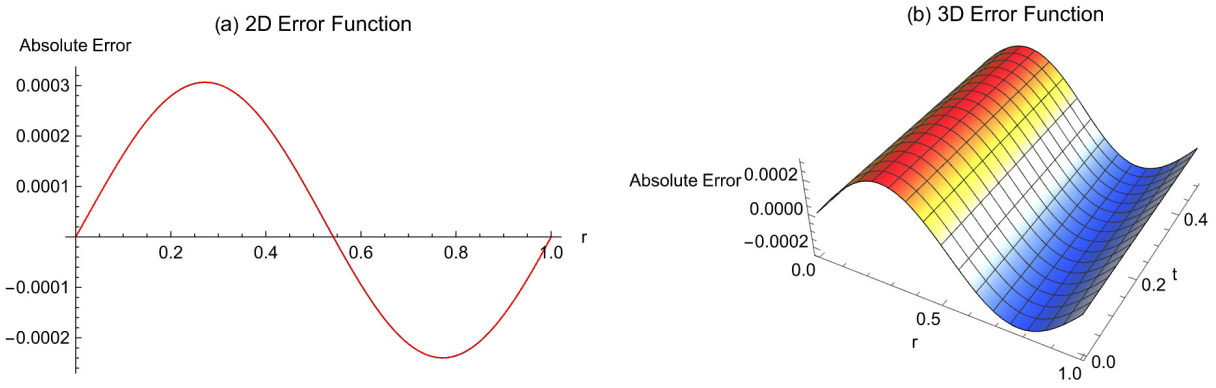

Figure 7. 2D and 3D error plot of Example 3 at $N = 100$, $\alpha = 0.45, T = 0.1,\ \beta = 0.000025, \triangle t = 0.002$.

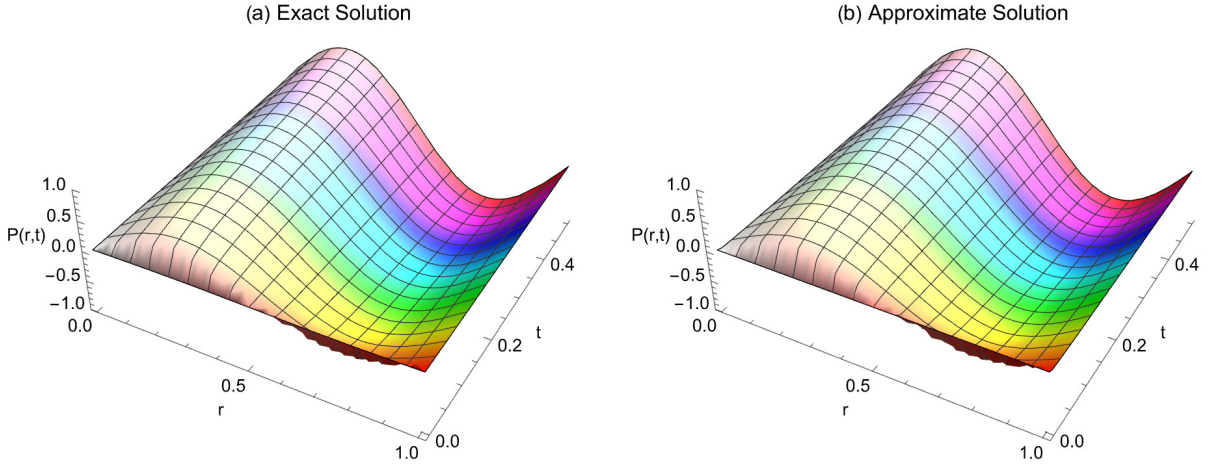

Figure 8. A 3D plot of the exact and approximate solutions when $\alpha = 0.25,\ T = 1$, and $r \in [0, 1]$ for Example 3.

7. Numerical examples

7.1. Example 1

Consider the following TFCDRE

$$\frac{\partial^\alpha p(r,t)}{\partial t^\alpha} + \frac{1}{(1+r)}\frac{\partial p(r,t)}{\partial r} - \frac{\partial^2 p(r,t)}{\partial r^2} - (1+2r)^2 p(r,t) = g(r,t), \quad r \in [0,1],\ t \in [0,1], \quad (45)$$

with the source term

$$g(r,t) = (1+t^{3+\alpha})\left(\frac{4}{1+r} - r(2-r)(1+2r)^2\right) + \frac{1}{6}\Gamma(4+\alpha)t^3 r(2-r),$$

the exact solution [14]

$$p(r,t) = (1+t^{3+\alpha})r(2-r),$$

the initial and end conditions

$$\varphi_1(r) = r(2-r),\ \varphi_2(t) = 0,\ \varphi_3(t) = (1+t^{3+\alpha}).$$

The piecewise polynomial can be achieved by the general Eq. (8) as:

$$P(r,t) = S^n_{j-1}B_{j-1}(r) + S^n_j B_j(r) + S^n_{j+1}B_{j+1}(r). \quad (46)$$

$$P(r,1) = \begin{cases} -1.93040E-13 + 4.00010r - 1.99995r^2 + 0.00206891r^3 - 0.109997r^4, & r \in [0.00, 0.01), \\ -4.39874E-09 + 4.00010r - 2.00008r^2 + 0.00646746r^3 - 0.109997r^4, & r \in [0.01, 0.02), \\ -3.95869E-08 + 4.00011r - 2.00035r^2 + 0.010866r^3 - 0.109997r^4, & r \in [0.02, 0.03), \\ -1.58346E-07 + 4.00012r - 2.00074r^2 + 0.0152645r^3 - 0.109997r^4, & r \in [0.03, 0.04), \\ \vdots & \vdots \\ -0.00715252 + 4.05676r - 2.16823r^2 + 0.222026r^3 - 0.110011r^4, & r \in [0.50, 0.51), \\ -0.0077364 + 4.06019r - 2.17496r^2 + 0.226428r^3 - 0.110011r^4, & r \in [0.51, 0.52), \\ -0.00835533 + 4.06376r - 2.18183r^2 + 0.23083r^3 - 0.110011r^4, & \in [0.052, 0.53) \\ \vdots & \vdots \\ -0.103823 + 4.42157r - 2.64144r^2 + 0.433711r^3 - 0.110015r^4, & r \in [0.98, 0.99), \\ -0.108111 + 4.43456r - 2.65457r^2 + 0.438129r^3 - 0.110014r^4, & r \in [0.99, 1.00). \end{cases} \quad (47)$$

Eq. (47) showcases the piecewise polynomial solution of section 7.1 when $N = 100$, $\alpha = 0.3$, $\triangle t = 0.01$, $\beta = 0.000011$, $T = 1$. Table 1 illustrates the comparison of the exact and approximate solutions of section 7.1 choosing $N = 80, 100$, and $\alpha = 0.35, 0.65$. The obtained exact and numerical results are in great agreement without exception. Also, β is a free parameter, and the values were arbitrarily chosen in all the experiments. Table 2 showcases the absolute numerical errors for section 7.1 when $N = 100$, $\triangle t = 0.01$, $\beta = 0.000055$, $T = 1$, and different values of α. In Table 3, we illustrate the Euclidean L_2

norms, the maximum absolute errors L_∞, and the order of convergence for section 7.1 when we set $T = 1$. Our results were compared with results mentioned in Ref. [14]. Table 4 illustrates the absolute error norms and the order of convergence when $\triangle t = 0.002$ and $T = 0.5$ for section 7.1. Our results were compared with results mentioned in Ref. [14]. In Table 5, we present the approximate solutions when time $T = 1$, $\alpha = 0.25, \triangle t = 0.001, \beta = 0.000055$, and different values of N.

Figure 1 showcases the $2D$ graph of the exact and approximate solutions for $N = 32$, $\triangle t = 0.01$, $\alpha = 0.45$, and $\beta = 0.000018$ at different time levels. Figure 2 represents the 2D and 3D error plot when $N = 100$, $\triangle t = 0.01$, $\alpha = 0.25$, and $\beta = 0.0000357$. Figure 3 illustrates a $3D$ comparison between the exact and approximate solution when $N = 80$, $\alpha = 0.35$, $\triangle t = 0.01, \beta = 0.0000141$, and $T = 1$.

7.2. Example 2

Consider the following TFCDRE

$$\frac{\partial^\alpha p(r,t)}{\partial t^\alpha} + \frac{\partial p(r,t)}{\partial r} - \frac{\partial^2 p(r,t)}{\partial r^2} + p(r,t) = g(r,t), \quad (r,t) \in (0,1)\times(0,1), \quad (48)$$

with the source term

$$g(r,t) = (4\pi^2+1)t^2\sin(2\pi r) + 2\pi t^2\cos(2\pi r) + \frac{2t^{2-\alpha}}{\Gamma(3-\alpha)}\sin(2\pi r),$$

the exact solution [16]

$$p(r,t) = t^2\sin(2\pi r),$$

the initial and end conditions

$$p(r,0) = 0,\ p(0,t) = p(1,t) = 0$$

.

$$P(r,1) = \begin{cases} 1.91729EE - 13 + 6.28131r - 0.00093591r^2 - 41.3152r^3 - 0.0173787r^4, & r \in [0.00, 0.01), \\ -1.64906E - 07 + 6.28136r - 0.0058935r^2 - 41.1493r^3 - 0.0520152r^4, & r \in [0.01, 0.02), \\ -2.79723E - 06 + 6.28176r - 0.0256772r^2 - 40.8182r^3 - 0.0864464r^4, & r \in [0.02, 0.03), \\ -0.0000160777 + 6.28309r - 0.0700375r^2 - 40.3233r^3 - 0.120536r^4, & r \in [0.03, 0.04), \\ \vdots & \vdots \\ -1.63081 + 22.4816r - 57.7246r^2 + 38.4762r^3 + 0.187155r^4, & r \in [0.55, 0.56), \\ -1.45831 + 21.5519r - 56.0441r^2 + 37.4397r^3 + 0.219422r^4, & r \in [0.56, 0.57), \\ -1.24847 + 20.4417r - 54.0759r^2 + 36.2529r^3 + 0.250823r^4, & r \in [0.57, 0.58), \\ \vdots & \vdots \\ 34.6473 - 116.568r + 122.999r^2 - 41.1644r^3 + 0.0863935r^4, & r \in [0.97, 0.98) \\ 34.9244 - 117.384r + 123.765r^2 - 41.3576r^3 + 0.0519618r^4, & r \in [0.98, 0.99), \\ 35.0505 - 117.732r + 124.049r^2 - 41.3847r^3 + 0.0173251r^4, & r \in [0.99, 1.00). \end{cases} \quad (49)$$

The piecewise polynomial of section 7.2 when $N = 100$, $\alpha = 0.3$, $\triangle t = 0.01$, $\beta = 0.000056$ is expressed in Eq. (49). Table 6 showcases the error norms, the order of convergence and CPU time at $\beta = 0.000121$, $\triangle t = 0.002$ comparing with the results given by Li and Wang [16]. The results confirm that the experimental rate of convergence of the proposed technique corresponds with the theoretical appraisals. Table 7 demonstrates the error norms at different time levels. Table 8 illustrates the comparison of the exact and approximate solutions at different values of r with $\alpha = 0.65$, $\beta = 0.000121$, $\triangle t = 0.001$, and time $T = 1$. In Table 9, we present the absolute errors when $\alpha = 0.35$, $\beta = 0.000045$, $\triangle t = 0.002$, at different time intervals. Figure 4 demonstrates the $2D$ graph of the exact and approximate solutions with $\alpha = 0.5$, $\beta = 0.000144$, $\triangle t = 0.01$, and $N = 100$. Figure 5 showcases the 2D and 3D error plot when $\alpha = 0.5$, $\beta = 0.000044$, $\triangle t = 0.01$, $N = 100$. Figure 6 illustrates the $3D$ comparison between the exact and approximate solution given $N = 90$, $\alpha = 0.25$, $\triangle t = 0.01$, $T = 1$, and $\beta = 0.000025$.

7.3. Example 3

Consider the following TFCDRE

$$\frac{\partial^\alpha p(r,t)}{\partial t^\alpha} + \frac{\partial p(r,t)}{\partial r} - \frac{\partial^2 p(r,t)}{\partial r^2} + p(r,t) = g(r,t), \quad (r,t) \in (0,1)\times(0,1], \quad (50)$$

with the source term

$$g(r,t) = \left(\Gamma(\alpha+1) + \frac{6t^{3-\alpha}}{\Gamma(4-\alpha)}\right)\sin(2\pi r) + (4\pi^2+1)(t^\alpha + t^3)\sin(2\pi r) + 2\pi(t^\alpha + t^3)\cos(2\pi r),$$

the exact solution

$$p(r,t) = (t^\alpha + t^3)\sin(2\pi r),$$

the initial and end conditions

$$p(r,0) = 0,\ p(0,t) = p(1,t) = 0.$$

$$P(r,t) = \begin{cases} 1.73559E - 13 + 4.92938r - 0.000687003r^2 - 32.4228r^3 - 0.0294656r^4, & r \in [0.00, 0.01), \\ -1.30988E - 07 + 4.92942r - 0.00463426r^2 - 32.29r^3 - 0.0881974r^4, & r \in [0.01, 0.02), \\ -2.22191E - 06 + 4.92973r - 0.0203862r^2 - 32.0251r^3 - 0.146581r^4, & r \in [0.02, 0.03), \\ -0.0000127709 + 4.93079r - 0.0557055r^2 - 31.6292r^3 - 0.204386r^4, & r \in [0.03, 0.04), \\ \vdots & \vdots \\ -1.13182 + 16.3146r - 41.82r^2 + 27.6837r^3 - 0.5265r^4, & r \in [0.40, 0.41), \\ -1.20705 + 16.8616r - 43.1376r^2 + 28.7142r^3 - 0.476812r^4, & r \in [0.41, 0.42), \\ -1.27952 + 17.3754r - 44.3426r^2 + 29.6272r^3 - 0.425242r^4, & r \in [0.42, 0.43), \\ \vdots & \vdots \\ 27.4523 - 92.3004r + 97.4028r^2 - 32.6428r^3 + 0.088113r^4, & r \in [0.98, 0.99), \\ 27.5222 - 92.4554r + 97.4442r^2 - 32.5404r^3 + 0.0293808r^4, & r \in [0.99, 1.00). \end{cases} \quad (51)$$

The piecewise polynomial of section 7.3 when $N = 100$, $\alpha = 0.6$, $\triangle t = 0.01$, $\beta = 0.0000121$, and $T = 1$ is represented in Eq. (51). Table (10) demonstrates the approximate solutions when $\beta = 0.000062$, $\triangle t = 0.01$, and $T = 1$ for Example 3. Table 11 illustrates the error norms and the convergence order when $\triangle t = 0.004$, $\beta = 0.000015$, and time $T = 1$. In Table 12, we showcase the maximum absolute errors at $\beta = 0.000091$ and $\triangle t = 0.004$. Figure 7 depicts the 2D and 3D error plot when $N = 100$, $\alpha = 0.45$, $\beta = 0.000025$, $\triangle t = 0.002$. Figure 8 illustrates a $3D$ plot of the exact and approximate solution for $N = 70$, $\alpha = 0.25$, $\triangle t = 0.004, \beta = 0.000051$, and time $T = 1$.

8. Conclusion

In this study, an efficient numerical technique that is based on ExCBS for determining the TFCDRE is presented. This technique is a combination of Caputo's formulation and the

ExCBS. The CFD has been discretized employing the conventional finite difference method. We demonstrate that the temporal discretization is unconditionally stable, and the numerical solutions converge to the exact solutions with convergence order of $O(h^2 + \triangle t^{2-\alpha})$, where $\triangle t$ represents the temporal step size. The extended CBS collocation method is highly accurate for the given problems. The three experimental results were performed by employing the suggested technique and graphically (2D and 3D) presented to confirm the feasibility and accuracy of the scheme. The accuracy was further tested by varying the values of parameters N, $\triangle t$, β and T. The method is more valid and accurate for different values of the fractional order α when compared with existing results.

Acknowledgment

The authors sincerely thank everyone who has played a role in the success of this research project and all anonymous references cited in the work.

References

[1] R. Hilfer, *Applications of fractional calculus in physics*, World Scientific Publishing Co. Pte, Singapore, 2000. https://cir.nii.ac.jp/crid/1361137044225841024.

[2] A. Ahmadova & N. I. Mahmudov, "Langevin differential equations with general fractional orders and their applications to electric circuit theory", Journal of Computational and Applied Mathematics **388** (2021) 113299. https://doi.org/10.1016/j.cam.2020.113299.

[3] R. O. Awonusika & O. A. Mogbojuri, "Approximate analytical solution of fractional lane-emden equation by mittag-leffler function method", Journal of the Nigerian Society of Physical Sciences **4** (2022) 265. https://doi.org/10.46481/jnsps.2022.687.

[4] K. A. Abro, A. Siyal, A. Atangana & Q. M. Al-Mdallal, "Analytical solution for the dynamics and optimization of fractional Klein–Gordon equation: an application to quantum particle", Optical and Quantum Electronics **55** (2023) 704. https://doi.org/10.1007/s11082-023-04919-1.

[5] A. A. Kilbas, H. M. Srivastava & J. J. Trulillo, *Theory and applications of fractional differential equations*, J. van Mill, Ed. Amsterdam: Elsevier, 2006. https://digital.library.tu.ac.th/tu_dc/frontend/Info/item/dc:17558.

[6] K. M. Owolabi, A. Atangana & A. Akgul, "Modelling and analysis of fractal-fractional partial differential equations: application to reaction diffusion model", Alexandria Engineering Journal **5** (2020) 2477. https://doi.org/10.1016/j.aej.2020.03.022.

[7] A. O. Yunus & M. O. Olayiwola, "The analysis of a novel COVID-19 model with the fractional-order incorporating the impact of the vaccination campaign in Nigeria via the Laplace-Adomian Decomposition Method", Journal of the Nigerian Society of Physical Sciences (2024) 1830. https://doi.org/10.46481/jnsps.2024.1830.

[8] J. Rashidinia, A. Momeni & M. Molavi-Arabshahi, "Solution of convection-diffusion model in groundwater pollution", Scientific Reports **14** (2024) 2075. https://doi.org/10.1038/s41598-024-52393-w.

[9] G. S. Teodoro, J. T. Machado & E. C. De Oliveira, "A review of definitions of fractional derivatives and other operators", Journal of Computational Physics **388** (2019) 195. https://doi.org/10.1016/j.jcp.2019.03.008.

[10] A. S. Hendy & M. A. Zaky, "A priori estimates to solutions of the time-fractional convection–diffusion–reaction equation coupled with the Darcy system", Communications in Nonlinear Science and Numerical Simulation **109** (2022) 106288. https://doi.org/10.1016/j.cnsns.2022.106288.

[11] P. Prakash, K. Priyendhu & K. Anjitha, "Initial value problem for the (2+ 1)-dimensional time-fractional generalized convection–reaction– diffusion wave equation: invariant subspaces and exact solutions", Computational and Applied Mathematics **41** (2022) 30. https://doi.org/10.1007/s40314-021-01721-1.

[12] E. F. Anley, M. Basha, A. Hussain & B. Dai, "Numerical simulation for nonlinear space-fractional reaction convection-diffusion equation with its application", Alexandria Engineering Journal **65** (2023) 245. https://doi.org/10.1016/j.aej.2022.10.047.

[13] V. R. Hosseini, A. A. Mehrizi, H. Karimi-Maleh & M. Naddafi, "A numerical solution of fractional reaction–convection–diffusion for modeling PEM fuel cells based on a meshless approach", Engineering Analysis with Boundary Elements **155** (2023) 707. https://doi.org/10.1016/j.enganabound.2023.06.016.

[14] Y.-M. Wang & L. Ren, "Efficient compact finite difference methods for a class of time-fractional convection–reaction–diffusion equations with variable coefficients", International Journal of Computer Mathematics, **96** (2019) 264. https://doi.org/10.1155/2019/7969371.

[15] C.-S. Liu & C.-W. Chang, "Collocation method with fractional powers exponential trial functions for singularly perturbed reaction convection-diffusion equation", International Journal of Thermal Sciences **146** (2019) 106070. https://doi.org/10.1016/j.ijthermalsci.2019.106070.

[16] C. Li & Z. Wang, "Numerical methods for the time fractional convection-diffusion-reaction equation", Numerical Functional Analysis and Optimization **42** (2021) 1115. https://doi.org/10.1080/01630563.2021.1936019.

[17] S. Toprakseven, "A weak Galerkin finite element method for time fractional reaction-diffusion-convection problems with variable coefficients", Applied Numerical Mathematics **168** (2021) 1. https://doi.org/10.1016/j.apnum.2021.05.021.

[18] E. Ngondiep, "A two-level fourth-order approach for timefractional convection–diffusion–reaction equation with variable coefficients", Communications in Nonlinear Science and Numerical Simulation **111** (2022)106444. https://doi.org/10.1016/j.cnsns.2022.106444.

[19] R. Choudhary, S. Singh & D. Kumar, "A second-order numerical scheme for the time-fractional partial differential equations with a time delay", Computational and Applied Mathematics **41** (2022) 114. https://doi.org/10.1007/s40314-022-01810-9.

[20] M. Naeem, N. H. Aljahdaly, R. Shah & W. Weera, "The study of fractional-order convection-reaction-diffusion equation via an Elzake Atangana-Baleanu operator", AIMS Math **7** (2022) 18. https://doi.org/10.3934/math.2022995.

[21] H. Yasmin, "Application of Aboodh homotopy perturbation transform method for fractional-order convection–reaction–diffusion equation within caputo and atangana–baleanu operators", Symmetry bf15 (2023) 453. https://doi.org/10.3390/sym15020453.

[22] Y. Zhang & M. Feng, "The virtual element method for the time fractional convection diffusion reaction equation with non-smooth data", Computers & Mathematics with Applications **110** (2022) 1. https://doi.org/10.1016/j.camwa.2022.01.033.

[23] F. M. Salama, N. Hj. Mohd. Ali & N. N. Abd Hamid, "Efficient hybrid group iterative methods in the solution of two-dimensional time fractional cable equation", Advances in Difference Equations **2020** (2020) 257. https://doi.org/10.1186/s13662-020-02717-7.

[24] F. M. Salama, N. N. Abd Hamid, N. H. M. Ali & U. Ali, "An efficient modified hybrid explicit group iterative method for the time-fractional diffusion equation in two space dimensions", AIMS Mathematics bf7 (2022) 2370. https://doi.org/10.3934/math.2022134.

[25] M. Basim, N. Senu, A. Ahmadian, Z. Ibrahim, and S. Salahshour, "Solving fractional variable-order differential equations of the non-singular derivative using Jacobi operational matrix", Journal of the Nigerian Society of Physical Sciences **2** (2023) 1221. https://www.journal.nsps.org.ng/index.php/jnsps/article/view/1221.

[26] L. Yan, S. Kumbinarasaiah, G. Manohara, H. M. Baskonus, and C. Cattani, "Numerical solution of fractional PDEs through wavelet approach", Zeitschrift f¨ur angewandte Mathematik und Physik **75** (2024) 61. https://link.springer.com/article/10.1007/s00033-024-02195-x.

[27] K. Issa, R. A. Bello, and U. J. Abubakar, "Approximate analytical solution of fractional-order generalized integro-differential equations via fractional derivative of shifted Vieta-Lucas polynomial", Journal of the Nigerian Society of Physical Sciences (2024) 1821. https://doi.org/10.46481/jnsps.2024.1821.

[28] H. Eltayeb, "Application of double Sumudu-generalized Laplace decomposition method and two-dimensional time-fractional coupled Burger's equation", Boundary Value Problems **2024** (2024) 48. https://doi.org/10.1186/s13661-024-01851-5.

[29] R. Pant, G. Arora, B. K. Singh, and H. Emadifar, "Numerical solution of two-dimensional fractional differential equations using Laplace transform with residual power series method", Nonlinear Engineering, **13** (2024) 20220347. https://doi.org/10.1515/nleng-2022-0347.

[30] M. Yaseen and M. Abbas, "An efficient computational technique based on cubic trigonometric B-splines for time fractional Burgers' equation", International Journal of Computer Mathematics **97** (2020) 725. https://doi.org/10.1080/00207160.2019.1612053.

[31] M. Shafiq, M. Abbas, K. M. Abualnaja, M. Huntul, A. Majeed & T. Nazir, "An efficient technique based on cubic B-spline functions for solving time-fractional advection diffusion equation involving Atangana–Baleanu derivative", Engineering with Computers, pp. 1–17, 2021. https://doi.org/10.1007/s00366-021-01490-9.

[32] P. Roul, V. Rohil, G. Espinosa-Paredes, and K. Obaidurrahman, "An efficient numerical method for fractional neutron diffusion equation in the presence of different types of reactivities", Annals of Nuclear Energy **152** (2021) 108038. https://www.sciencedirect.com/science/article/abs/pii/S0306454920307349.

[33] A. A. Okeke, N. N. A. Hamid, and M. Abbas, "A numerical technique for solving time-fractional Navier-Stokes equation with Caputo's derivative using cubic B-spline functions", in *AIP Conference Proceedings*, AIP Publishing, 2024. https://doi.org/10.1063/5.0193362.

[34] P. Roul and V. P. Goura, "A high-order B-spline collocation scheme for solving a nonhomogeneous time-fractional diffusion equation", Mathematical Methods in the Applied Sciences **44** (2021) 546. https://doi.org/10.1002/mma.6760.

[35] M. Abbas, A. Bibi, A. S. Alzaidi, T. Nazir, A. Majeed, and G. Akram, "Numerical solutions of third-order time-fractional differential equations using cubic B-Spline functions", Fractal and Fractional **6** (2022) 528. https://doi.org/10.3390/fractalfract6090528.

[36] A. Umer, M. Abbas, M. Shafiq, F. A. Abdullah, M. De la Sen, and T. Abdeljawad, "Numerical solutions of atangana-baleanu time-fractional advection diffusion equation via an extended cubic b-spline technique", Alexandria Engineering Journal bf74 (2023) 285. https://doi.org/10.1016/j.aej.2023.05.028.

[37] A. R. Hadhoud, A. A. Rageh, and T. Radwan, "Computational solution of the time-fractional schr¨odinger equation by using trigonometric bspline collocation method", Fractal and Fractional **6** (2022) 127. https://doi.org/10.3390/fractalfract6030127.

[38] T. Akram, A. Iqbal, P. Kumam, and T. Sutthibutpong, "Investigation of the fractional coupled-Burgers model with the exponential kernel", Ain Shams Engineering Journal **15** (2024) 102450. https://doi.org/10.1016/j.asej.2023.102450.

[39] U. Ghafoor, M. Abbas, T. Akram, E. K. El-Shewy, M. A. Abdelrahman & N. F. Abdo, "An efficient cubic b-spline technique for solving the time fractional coupled viscous burgers equation", Fractal and Fractional **8** (2024) 93. https://doi.org/10.3390/fractalfract8020093.

[40] F. Mirzaee & S. Alipour, "Cubic B-spline approximation for linear stochastic integro-differential equation of fractional order", Journal of Computational and Applied Mathematics **366** (2020) 112440. https://www.sciencedirect.com/science/article/pii/S0377042719304431.

[41] B. Khan, M. Abbas, A. S. Alzaidi, F. A. Abdullah & M. B. Riaz, "Numerical solutions of advection diffusion equations involving Atangana–Baleanu time fractional derivative via cubic B-spline approximations", Results in Physics **42** (2022) 105941. https://www.sciencedirect.com/science/article/pii/S2211379722005605.

[42] S. U. Arifeen, S. Haq & F. Golkarmanesh, "Computational study of multiterm time-fractional differential equation using cubic B-spline finite element method", Complexity **2022** (2022) 3160725. https://doi.org/10.1155/2022/3160725.

[43] B. Cao, X. Wu, Y. Wang & Z. Zhu, "Modified hybrid B-spline estimation based on spatial regulator tensor network for burger equation with nonlinear fractional calculus", Mathematics and Computers in Simulation **220** (2024) 253. https://www.sciencedirect.com/science/article/abs/pii/S0378475424000156.

[44] S. K. Sahoo, P. O. Mohammed, H. M. Srivastava, A. Kashuri, N. Chorfi & D. Baleanu, "Computational analysis of time fractional diffusion wave equation via novel B-splines-based technique", AIMS Mathematics **9** (2024) 751. .

[45] I. Podlubny, *Fractional differential equations: an introduction to fractional derivatives, fractional differential equations, to methods of their solution and some of their applications*, Elsevier, 1998. https://pascal-francis.inist.fr/vibad/index.php?action=getRecordDetail&idt=63919.

[46] J. R. Poulin, *Calculating infinite series using Parseval's identity*, The University of Maine, 2020. https://digitalcommons.library.umaine.edu/etd/3196/.

[47] H. Xuli, "An extension of the cubic uniform B-spline curve", Journal of Computer Aided Design and Computer Graphics **15** (2003) 576.

[48] Y. Lin & C. Xu, "Finite difference/spectral approximations for the time-fractional diffusion equation", Journal of computational physics **225** (2007) 1533. https://doi.org/10.1016/j.jcp.2007.02.001.

[49] S. Daochun, G. Zhendong, L. Weiqun & Y. Chao, "The order of complex numbers", arXiv preprint **9** (2010). https://doi.org/10.48550/arXiv.1003.4906.

[50] M. K. Kadalbajoo & P. Arora, "B-spline collocation method for the singular-perturbation problem using artificial viscosity", Computers & Mathematics with Applications **57** (2009) 650. https://doi.org/10.1016/j.camwa.2008.09.008.

[51] C. de Boor, "On the convergence of odd-degree spline interpolation", Journal of approximation theory **1** (1968) 452. https://core.ac.uk/download/pdf/82288008.pdf.

[52] C. Hall, "On error bounds for spline interpolation", Journal of approximation theory **1** (1968) 209. https://doi.org/10.1016/0021-9045(68)90025-7.